The Environmental Costs of Sanctions: Flaring and Venting in Venezuela*

Michele Fioretti† Kavanaugh FitzPatrick‡ Alessandro Iaria§

July 2026

Abstract

Economic sanctions on oil-producing autocracies change not only the quantity of oil but also how it is produced. Combining field-level production data with satellite measurements of gas flaring and atmospheric methane across six Latin American countries from 2012 to 2024, we study the U.S. sanctions on Venezuela. Per-barrel gas flaring in Venezuela rose about two-and-a-half-fold even as production fell by two-thirds—a pattern no unsanctioned neighbor shows—so environmental damage under sanctions is about two and a half times what a proportional decline in output would predict. Three channels generate this gap: the exit of small, dirty fields (composition) is more than offset by surviving fields running their infrastructure past design capacity (strain) and cutting their operating budgets (maintenance). We identify strain from the response of satellite-measured methane to the world price of naphtha, the imported diluent Venezuela's extra-heavy crude requires, and maintenance from a November 2022 U.S. Treasury license that allowed only Chevron to resume operations at its Venezuelan fields. A similar pattern of rising per-barrel emissions despite falling output appears under the sanctions on Iran (after 2018).

JEL Classification: F51, Q53, Q35, L71

Keywords: Sanctions, gas flaring, methane, venting, Venezuela, oil production, environmental externalities, Orinoco Belt

*Fioretti and Iaria gratefully acknowledge funding from the British Academy/Leverhulme Small Research Grants Scheme (grant number SRG2324/240698). The study was also funded by the European Research Council (ERC Starting Grant 101221025 – BALANCE). All errors are ours.

†Università Bocconi, Department of Economics, IGIER, and CEPR. E-mail: fioretti.m@unibocconi.it

‡Università Bocconi, Department of Economics. E-mail: kavfitzpatrick@gmail.com.

§University of Bristol, School of Economics, and CEPR. E-mail: alessandro.iaria@bristol.ac.uk

1 Introduction

Economic sanctions are among the most widely used instruments of foreign policy. Their environmental consequences, however, are poorly understood. When sanctions target an oil-producing state, the policy calculus weighs geopolitical aims against the humanitarian cost of lost output. It rarely weighs how the remaining oil is produced. Yet oil extraction is infrastructure-intensive. Wells, pipelines, compressors, and gas-handling plants need sustained investment, imported equipment, and technical expertise to run within environmental limits. Sanctions cut off the inputs that keep this infrastructure working. The result need not be only a reduction in output. It can also be a degradation of the production process itself, so that the remaining barrels become not merely fewer but more emissions-intensive.

Venezuela offers a useful setting in which to study this degradation. In August 2017 the United States imposed financial sanctions on Venezuela's government and its state oil company, PDVSA. In January 2019 it cut PDVSA off from the dollar system and from naphtha, the light petroleum product used to thin Venezuela's tar-like crude so it can flow through a pipeline. Venezuelan oil output then fell by about two-thirds (U.S. Energy Information Administration, 2024; Monaldi et al., 2021), but the gas *flared* (burned off at the wellhead rather than captured) did not fall with it. We build a field-level panel of six Latin American oil producers over 2012–2024, pairing production records with satellite measurements of flaring (the World Bank's VIIRS night-time product) and atmospheric methane (the Sentinel-5P TROPOMI sensor). Flaring per barrel of Venezuelan oil rose from 20.3 to 48.1 cubic meters between the pre-sanctions years and 2022–2024, a factor of about 2.4. Total flaring damage therefore declined only modestly, even as output collapsed. No other country in the panel shows this. Colombia's crude slate also shifted toward heavy oil, yet its flaring per barrel fell by more than half.

This paper investigates why pollution per barrel rose following the sanctions. We split the rise into three channels—composition, strain, and maintenance—each tied to a distinct policy lever. Composition is about which fields produce: when sanctions raise the fixed cost of operating a field, production tilts toward the survivors, which may be cleaner or dirtier per barrel than the fields that exit. Strain is about how intensively the surviving infrastructure runs: as the pipes and plants that handle the gas are pushed past the capacity they were built for, more of the gas that comes up with the oil is vented or flared instead of captured. Maintenance is about how well each barrel is produced: when upkeep of compressors and gas-capture equipment is deferred, emissions rise at a given level of output. The three channels are exhaustive (which fields operate, how much each produces, and how each is run) and they are easy to confuse, because any pollution measure responds to all three at once. Separating them is the central task, and we study each with a design that holds the other two fixed. The gas can leave a field in two forms, and the form it takes matters: flared, it burns into carbon dioxide; vented, it escapes as methane, which does far more climate damage and is invisible to the satellites that track flaring.

The strain channel is the paper's central result. Venezuela's extra-heavy crude is too thick to flow through a pipeline unless it is thinned with naphtha, bought on world markets. Its price is therefore set far from Venezuela and cannot be moved by the methane over any one Venezuelan field. When naphtha is expensive, the diluent that keeps the crude moving runs short, and gas escapes as the handling chain strains to cope. The clearest case is a substitution: to stretch the scarce import, operators thin the extra-heavy crude with lighter crude drawn from Venezuela's eastern conventional fields. Those fields carry far more gas per barrel, and the compressors that once pumped that gas back underground have failed, so working those fields harder to supply diluent vents their gas as methane.

We track how the methane measured above each 10 km patch of ground moves with the world naphtha price, holding fixed each patch's own baseline and the conditions common to a month. It rises where this mechanism operates: along the pipeline corridor that carries the diluted crude and at the conventional fields pulled into the blend, but not along the matching corridor for crude that flows on its own, nor at the extra-heavy wells, whose oil carries almost no gas. The methane responds only where the mechanism is present, and only in Venezuela, which distinguishes the channel from any common oil-price swing.

The composition channel pushes average pollution per barrel down rather than up, against the intuition that a collapsing oil sector tilts toward a more emissions-intensive mix. Surviving Venezuelan production shifted toward the resource-rich, extra-heavy core in the country's east, kept running by the foreign partners who stayed: PetroPiar with Chevron, Sinovensa with China's CNPC, and the Indian-run Carabobo block. It shifted away from the conventional fields PDVSA was left to run alone, which carry far more gas per barrel and so flare more, all else equal. Moving the average barrel toward the extra-heavy core therefore lowers the gas flared per barrel. Composition is an offset: the rise happens despite a favorable shift in the mix, which makes the within-field deterioration behind it larger still.

The sanctions themselves supplied the experiment we need for the maintenance channel. In November 2022 the U.S. Treasury issued a license, General License (G.L.) 41, that let Chevron (and only Chevron) resume operating its Venezuelan fields while still barring any payment to the government (Congressional Research Service, 2024). It restored the spare parts, expertise, and financing for upkeep at a handful of fields without restoring revenue to the regime. The fields left out, together with the years before the license, show what would have happened without it. The license raised maintenance spending at those fields, and in the flaring-volume regression a one-percent rise in per-barrel upkeep is associated with about 0.54 percent lower flaring volume. If anything, this understates the maintenance margin, since upkeep is measured as total operating spending per barrel, only part of which bears on gas handling; the response to abatement spending alone, the object that structural estimates such as Shapiro and Walker (2018) recover, would be larger.

We then add up the three channels. Composition, the favorable shift toward cleaner fields, subtracts 6.9 cubic meters per barrel (m^3/bbl); the two within-field forces more than offset it, strain adding 23.5 and deferred maintenance 11.2, a split the Chevron elasticity pins down. Valued at the U.S. Environmental Protection Agency's social costs of carbon and methane, the gas burned does about \$5 billion (bn) of climate damage a year and the gas vented about \$6 bn, some \$11 bn in all, or forty dollars for every barrel Venezuela still produces.[1] Those figures are levels, the sector's annual bill as sanctions have left it, not increments over a no-sanctions path; Section 8.2 separates the two where the data allow, putting the excess over proportional decline at roughly \$3 bn a year of the flaring bill and, under a single stated assumption, some \$4 bn of the venting bill. The mix of emissions shifted

[1]Flaring: our panel shows about 13.7 bn m^3 of gas flared a year over 2022–2024, in line with the World Bank tracker (World Bank, 2026); burned at roughly two kilograms of carbon dioxide per cubic meter, that is about 27 Mt (million metric tons) a year, or \$5 bn at the EPA central social cost of carbon of \$190 per metric ton (U.S. Environmental Protection Agency, 2023). Venting: the IEA inventory puts Venezuelan oil-and-gas methane near 3.6 Mt a year (International Energy Agency, 2025), or \$6 bn at the EPA social cost of methane of \$1,600 per metric ton (U.S. Environmental Protection Agency, 2023).

with the sanctions: output fell by two-thirds while the gas flared fell by only about a fifth, and the gas vented rose, unburned methane doing far more damage than the same gas burned off. This climate cost goes unrecorded in a policy debate that weighs sanctions in lost output and revenue, yet the part the sanctions caused, roughly \$7 bn a year, is more than two-fifths of the \$16 bn in lost oil revenue that synthetic-control estimates attribute to them (Rodríguez, 2022).

The strain and maintenance channels point to a policy remedy. Both depend on inputs the operator cannot buy under sanctions—the diluent that moves the crude and the spare parts and service contracts that hold emissions down—and both can be licensed apart from the revenue the sanctions are meant to deny. The Chevron license showed the separation works: it restored those inputs at four fields yet did not relax the ban on revenue to the regime, because the proceeds went to Chevron in repayment of debts the state firm owed it. A license written for the inputs of lower-emissions operation rather than for output, an *environmental carve-out*, would relieve the technical constraint that drives the within-field rise while leaving the financial one in place. Its value is a climate benefit the operator does not capture, the wedge between social and private returns (Bloom et al., 2013). Left to the market, the gap stays open: the state firm cannot fund the rebuild and the foreign firms that could are deterred by sanctions and by the risk of expropriation (Fioretti et al., 2026b).

The paper contributes to three literatures. The first measures what sanctions cost the countries they target: Hufbauer et al. (2007), Neuenkirch and Neumeier (2015), and Gutmann et al. (2023) assess their aggregate effects, Afesorgbor (2019) and Crozet and Hinz (2020) the trade losses, and a Venezuelan strand debates how much of the oil collapse the sanctions caused (Weisbrot and Sachs, 2019; Bahar et al., 2019; Rodríguez, 2022; Monaldi et al., 2021; Fernández-Villaverde et al., 2025). That work asks how much oil gets produced and sold. The paper asks how the oil that remains is produced, and shows that sanctions degrade the process, with environmental costs that the output figures do not record.

The second studies the aggregate consequences of distortions for the allocation of production: Restuccia and Rogerson (2008) and Hsieh and Klenow (2009) measure the productivity cost of misallocation, and later work extends the margin to industry cases and to the environment (Asker et al., 2014; Tombe and Winter, 2015; Fowlie et al., 2012; Graff, 2026). In our setting the welfare loss runs not through measured productivity but through external damage: the same barrel, produced with higher emissions intensity.

The third decomposes environmental performance into the margins that produce it. Shapiro and Walker (2018) split the fall in U.S. manufacturing pollution into scale, composition, and technique; Masnadi et al. (2018), Asker et al. (2024), Coulomb et al. (2026), and Covert and Kellogg (2025) study how the composition of oil supply sets its external damage; and a remote-sensing strand measures oil-and-gas pollution from orbit (Cust et al., 2017; Lade and Rudik, 2020; Agerton et al., 2023; Blundell and Kokoza, 2022; Plant et al., 2022; Lorente et al., 2021; Marks, 2022; Nathan et al., 2024). Our composition and within-field margins are the extraction analogue of composition and technique, estimated from orbit. The paper's contribution is to bring the three literatures together in one setting and to identify each channel with its own design: operator selection and gas–oil ratios for composition, a naphtha-price instrument for strain, and the Chevron license for maintenance.

The paper is structured as follows. Section 2 sets out the three-channel framework; Section 3 the sanctions chronology and the physics of extra-heavy oil; Section 4 the data and the descriptive rise. Sections 5 to 7 identify the composition, strain, and maintenance channels in turn. Section 8 adds up the channels, values them at the social cost of carbon and methane, develops the maintenance externality, and draws out the implications for sanctions design and the investment gap. Section 9 concludes. Robustness and supplementary material are collected in the Online Appendix.

2 Conceptual Framework

A natural benchmark for the environmental impact of a sanctions-induced output decline is *proportional decline*: if production falls by x percent, the damage from extraction (flaring, methane leakage, local pollutants) falls by x percent too. The benchmark presumes the production technology is unchanged: the same fields operate, each is run at unchanged operating intensity, and none is pushed past its design envelope. Whether it holds is the central empirical question of this paper. Let R denote the ratio of post- to pre-sanctions flaring damage per barrel; under the benchmark $R = 1$, and in Venezuela $R \approx 2.4$, as production-weighted flaring intensity rises from 20.3 to 48.1 m^3/bbl.

Sanctions can move outcomes away from the benchmark along three central margins,

$$D = \underbrace{\sum_{i \in \text{operating}}}_{\substack{\text{(i) } \textit{composition}\text{:} \\ \text{which fields operate}}} \Bigg[\underbrace{\alpha_i(m_i)}_{\substack{\text{(ii) } \textit{maintenance}\text{:} \\ \text{per-barrel intensity}}} \cdot q_i + \underbrace{\frac{\beta_i}{2} q_i^2}_{\substack{\text{(iii) } \textit{strain}\text{:} \\ \text{convex in output}}} \Bigg]. \tag{1}$$

Total damage sums, over the operating fields, a per-barrel intensity times output plus a convex term, and each piece is a channel. We illustrate each channel below and show the derivation of each term of (1) in Appendix A.

Composition is the set the sum in (1) runs over: sanctions raise the per-period fixed cost of running any field (evasion infrastructure, lost foreign expertise, premium pricing for sanctioned counterparties), so fields that cannot clear the higher threshold shut down and output concentrates on the survivors. Whether that raises or lowers aggregate intensity depends on the baseline intensity gap between the fields that exit and those that stay, which Section 5 resolves in favor of the lower-intensity survivors.

Maintenance is the per-barrel intensity $\alpha_i(m_i)$, not an engineering constant but a quantity that falls in the operating budget m_i, which repairs leaks, replaces worn equipment, and keeps associated gas captured rather than burned ($\alpha_i'(m_i) < 0$); sanctions cut that budget through limited access to spare parts, capital, and foreign contractors, raising intensity wherever production continues.

Strain is the convex term $\frac{\beta_i}{2} q_i^2$ ($\beta_i \geq 0$): the pipes, compressors, and gas-handling equipment that move the co-produced gas have a fixed capacity, so as a surviving field absorbs the output of exited fields and presses toward that capacity, a growing share of its gas is flared or vented rather than captured, and damage per barrel rises faster than output.

The proportional-decline benchmark obtains when sanctions shift only the overall scale of output, leaving the operating set, each field's maintenance budget, and every field's proximity to capacity unchanged.

The three margins are not independent. When sanctions raise the fixed cost of operating a field, the field that can no longer cover it is retired (composition), the survivor absorbs its output and presses toward its own capacity (strain), and if the survivor's upkeep is cut at the same time, its per-barrel intensity rises (maintenance).

Choosing which fields to run, and how hard to run each, is the production-portfolio problem of a multi-field operator under capacity constraints (Fioretti et al., 2026a). Because one shock moves the three together, no single pollution series separates them, which is why identification requires multiple shocks. The three designs that follow share no common assumption, so a threat to one is not a threat to the others.

The aggregate per-barrel intensity is the production-weighted average of the field intensities,

$$I \;=\; \sum_i s_i\, \iota_i, \qquad \iota_i \;=\; \alpha_i(m_i) + \tfrac{\beta_i}{2}\, q_i, \tag{2}$$

with s_i field i's share of production, so a change in I splits into a between-field term (composition) and a within-field term ($\Delta\iota_i \;=\; \Delta\alpha_i + \Delta(\tfrac{\beta_i}{2} q_i)$, maintenance plus strain). Section 5 implements this split, and Section 8 aggregates the channel estimates into R and values them.

3 Sanctions and the Physics of Extra-Heavy Oil

The sanctions–environment link in Venezuela runs through a specific physical mechanism that is not generic to oil extraction. This section sets out the two pieces of context the analysis draws on: the sanctions chronology, and the physics of extra-heavy crude that makes Venezuela depart from the proportional-decline benchmark while its neighbors do not.

3.1 Sanctions Chronology

Venezuela holds the world's largest proven oil reserves and produces from two regions with distinct crude. The *Maracaibo Basin* in the west produces conventional heavy crude (11–19° API) that flows through pipelines without modification. The *Orinoco Belt* in the east (the *Faja*) produces extra-heavy crude (8–10° API) so viscous at surface temperatures that it cannot move through a pipeline without first being blended with imported light hydrocarbons, most commonly naphtha; the east also holds conventional, lighter-crude fields around Maturín. Before sanctions, the Orinoco accounted for roughly 51 percent of national crude output and Maracaibo for roughly 30 percent (U.S. Energy Information Administration, 2024; Monaldi et al., 2021). The asymmetry in crude characteristics, and the Orinoco's dependence on imported diluent, is the physical reason for the patterns this paper documents.

The United States imposed sectoral financial sanctions in August 2017 (Executive Order 13808), restricting U.S.-person dealings in new debt and equity issued by the government and PDVSA. In January 2019 the Treasury's Office of Foreign Assets Control designated PDVSA itself, severing it from the dollar clearing system and from U.S.-sourced inputs, most consequentially the naphtha that Orinoco crude requires for transport. Secondary sanctions in 2020 widened the perimeter to non-U.S. counterparties. Aggregate production fell from a 2016 level near 2.28 million barrels per day to a 2020 trough of about 0.58 before stabilizing near 0.78 in 2023–2024. The collapse extended well beyond oil: real GDP fell by about three-quarters between 2013 and 2021, and roughly seven million people, nearly a quarter of the population, emigrated (Alvarez et al., 2022).

In November 2022 the Treasury issued G.L. 41, permitting Chevron to resume operations at its Venezuelan joint ventures under a continued ban on revenue distribution to PDVSA. A broader easing, G.L. 44 of October 2023, briefly relaxed sanctions on the whole sector before their partial reimposition in 2024.

3.2 The Emissions of the Venezuelan Oil Sector

What should emissions do when production falls in a well-run field? Flaring is engineered to be small in steady state: associated gas is captured for sale, reinjected, or used as on-site fuel, and flared only as a safety relief (World Bank, 2024, 2025). Methane leakage scales with the equipment in service and its upkeep (Marks, 2022; Plant et al., 2022): when COVID-19 cut activity in the Permian, the largest U.S. basin, methane fell roughly in proportion and reversed with the recovery (Lyon et al., 2021). Under proportional decline, then, flaring intensity holds near its baseline level and methane falls in line with output.

The benchmark fails in Venezuela because of how extra-heavy oil moves. Orinoco crude is too viscous to flow through a pipeline on its own: it is blended with naphtha, hauled north to the upgraders on the José coast (the plants that turn the blend into exportable synthetic crude), and the naphtha recovered there is piped back to the wellheads for reuse, a closed diluent circuit (True, 1998; Chang, 1998; Hernández and Monaldi, 2016). The 2019 designation cut off the U.S. naphtha it ran on (Monaldi et al., 2021; U.S. Energy Information Administration, 2024), and since heavy-oil wells cannot be throttled without permanent damage from wax and asphaltene precipitation, lifted crude waits for thinning while the sinks that would take its associated gas—the sales pipelines, the reinjection compressors, the upgraders—fail with the circuit. What cannot be captured is flared or vented.

Where the gas escapes is set by its own geography, not the crude's. The Faja crude that needs the naphtha carries almost no gas of its own, its gas–oil ratio essentially zero, a feature of Orinoco oil (True, 1998). The methane over the corridor is therefore not wellhead gas but the strained system's own emissions, released by the equipment strung along the route as the circuit backs up.[2]

The gas-rich fields are the conventional ones of the east, around Maturín, which the circuit reaches by a second route: their light crude is the domestic substitute for imported naphtha, blended with Faja extra-heavy to make Merey 16 (Hernández and Monaldi, 2016; Caracas Chronicles, 2024). When naphtha is expensive, operators draw harder on these fields, and their associated gas, which the idle reinjection compressors can no longer push back underground, escapes for lack of a sink (Bellorín, 2016; Mogollon, 2021; Incorrys, 2026). Maracaibo conventional grades, by contrast, flow without diluent and can be shut down without comparable damage.

4 Data

We assemble a field-level panel of the six Latin American oil economies and pair it with two satellite records and a world price. Field production, operating and capital spending, ownership, crude grade, and oil-in-place come from Rystad Energy's UCube, which tracks 7,333 fields across Argentina, Brazil, Colombia, Ecuador, Mexico, and Venezuela over 2012–2024, 666 of them Venezuelan.

Flaring is the World Bank's VIIRS night-time product. We link flare-site-years to Rystad fields in two steps: accepted field-name matches are assigned directly, and remaining sites are allocated across producing fields within a geographic buffer using production-weighted inverse-squared-distance weights with a 100-meter distance floor, falling back to pure inverse-squared-distance weights when

[2] Because pipelines are sealed, methane detected in cells along a pipeline corridor must originate from associated infrastructure (e.g., right-of-way equipment, pump stations, storage and gathering facilities, and co-located gas and fuel-gas lines) and scales with their operation and maintenance (Marks, 2022; Plant et al., 2022).

production is missing; Appendix B illustrates the matching and its geographic allocation in full. Motivated by field shapes, the default allocation uses a 15 km buffer, and allocated volume divided by Rystad production gives flaring per barrel.[3] Figure 1 maps the resulting field-level flaring intensity across the six countries: Venezuela's Orinoco Belt and Maracaibo Basin carry the densest and most intense flaring in Latin America, set well above every neighbor.

Methane is the Sentinel-5P TROPOMI column—the average methane concentration of the air column above each point—aggregated to 10 km cells by month from late 2018, with 1,280 Venezuelan cells matched to oil-field and pipeline activity. The naphtha price used in the strain analysis is the northwest-European spot benchmark, and pipeline geometry is the union of the OpenStreetMap and Global Energy Monitor networks. For VIIRS flaring we report descriptive sensitivity at the 7.5 and 15 km radii and decomposition robustness at 10 and 15 km; the methane designs vary the wellhead and pipeline radius from 10 to 50 km.

The two satellites see different things, and the difference is central to the paper. VIIRS detects the heat of a flame, so a flare is bright and precisely located, but gas vented uncombusted gives off no heat and is invisible to it. TROPOMI instead measures the methane column over a 10 km cell, capturing the vented gas VIIRS misses but localizing it far less precisely, and its record begins only in late 2018. The two are complements: VIIRS gives a long, precise series on combustion for the descriptive rise and the maintenance channel, and TROPOMI the venting on which the strain channel depends.

Venezuela is the largest heavy-oil producer in the hemisphere and the only sanctioned one, and it was the most emissions-intensive large heavy-oil operation there before sanctions began. Table 1 sets its pre-sanctions numbers beside its neighbors: Venezuelan fields hold an order of magnitude more oil in place (a mean of 1,017 against 15–225 mn barrels), flared roughly four to thirty-seven times more per barrel (136.1 m^3/bbl at 15 km against 3.7–30.3 elsewhere), and were half state-owned (52 percent national-oil-company share against 20–39). The rest of the paper examines what sanctions did to this operation.

[3] We use the June-2026 release of the Global Gas Flaring Tracker (World Bank, 2026), whose enhanced methodology (three NOAA satellites and a recalibrated flare-location catalogue) revises the 2012–2024 history upward relative to earlier releases.

Figure 1: Oil fields and flaring intensity across Latin America

Notes. Each point is a Rystad field in the six-country panel; filled points flared at least once over 2012–2024, with marker size proportional to mean non-zero flaring intensity (winsorized at the 99.5th percentile), and hollow points never flared. Flaring is the World Bank VIIRS volume allocated under the default 15 km field-allocation rule. Crude grade and field location are from Rystad UCube. Basemap from Natural Earth.

4.1 The Motivating Fact

Sanctions did not raise the gas Venezuela flared; they cut the oil it produced, and per-barrel pollution rose through the ratio. Figure 2 plots country-level flaring, flaring per barrel, production, and operating spending in their native units.[4] Venezuelan output falls by about two-thirds after 2017 while the five unsanctioned neighbors hold roughly flat, and spending falls with it; the flared volume ends the period at its 2012 level, about a fifth below its pre-sanctions average. Flaring per barrel is the ratio of the two, so a roughly flat numerator over a denominator that falls by two-thirds produces the rise. A country that burns four-fifths of the gas while pumping a third of the oil appears, per barrel, two and a half times more emissions-intensive. Whether gas management also deteriorated (through venting rather than capture) is a separate question the flat VIIRS series cannot settle, because VIIRS sees combustion and not venting; Section 6 settles it with regressions that use the

[4] Appendix Table B.1 puts a difference-in-differences behind each series, adding capital spending and reporting flaring at both the 10 and 15 km allocation radii.

Table 1: Descriptive statistics

	Argentina	Brazil	Colombia	Ecuador	Mexico	Venezuela
Panel (a): Geology & Reservoir						
Water depth (m)	520.8 (540.3)	134.0 (161.6)	410.3 (829.1)	336.8 (388.5)	-146.1 (808.3)	111.0 (173.4)
Reservoir depth (m)	1872.1 (767.7)	1427.8 (736.8)	2446.3 (1235.9)	2572.5 (650.7)	3219.1 (1902.0)	2293.2 (1137.6)
Porosity (%)	7.6 (8.6)	2.8 (6.4)	6.5 (8.8)	18.2 (3.2)	4.2 (7.0)	9.8 (12.7)
Temperature (°C)	60.4 (19.2)	50.3 (18.5)	74.2 (27.2)	78.9 (16.7)	88.1 (37.5)	72.3 (36.1)
OOIP (mn bbl)	106.9 (529.5)	14.7 (127.7)	63.8 (460.8)	224.8 (764.0)	130.8 (840.6)	1016.6 (5248.7)
Recovery factor (%)	35.1 (13.9)	31.7 (20.5)	28.5 (12.3)	24.7 (7.8)	45.7 (236.3)	32.1 (14.7)
Panel (b): Production & Economics (pre-period mean)						
Production (kbbl/d)	0.4 (1.7)	0.1 (0.9)	0.6 (5.7)	2.0 (7.1)	1.1 (12.3)	3.9 (20.3)
OPEX (mn USD)	4.8 (21.2)	1.3 (10.8)	4.8 (42.3)	4.7 (16.2)	6.0 (52.4)	18.2 (87.8)
CAPEX (mn USD)	6.9 (32.6)	1.0 (6.3)	5.0 (35.2)	9.1 (34.9)	6.1 (45.5)	14.0 (62.9)
NOC ownership share (%)	25.1 (40.8)	23.9 (42.0)	20.4 (36.7)	38.8 (47.7)	24.7 (42.7)	51.5 (41.3)
Panel (c): Field Counts						
Number of fields	1,313	1,502	1,455	265	2,132	666
Share onshore (%)	91.2%	100.0%	95.3%	95.8%	66.5%	79.9%
Panel (d): Flaring (pre-period mean, matched fields)						
Flaring intensity, 7.5 km (m^3/bbl)	22.0 (147.5)	5.3 (13.1)	6.8 (27.7)	4.5 (29.7)	36.4 (180.7)	327.7 (746.0)
Flaring intensity, 15 km (m^3/bbl)	19.0 (121.0)	3.7 (10.8)	5.1 (23.7)	3.8 (26.4)	30.3 (132.0)	136.1 (420.9)
Flaring volume, 7.5 km (mn m^3)	1.9 (5.8)	3.6 (13.7)	4.1 (8.4)	7.8 (16.9)	44.5 (158.5)	154.1 (518.5)
Flaring volume, 15 km (mn m^3)	1.4 (4.7)	2.4 (11.0)	3.1 (7.8)	5.6 (15.0)	32.4 (133.4)	151.9 (797.9)

Notes. Panel (a) reports field-level geological characteristics; Panel (b), pre-period (2012–2016) field-year averages; Panel (c) counts all fields in the Rystad upstream database by country; and Panel (d) conditions on the matched subsample of fields with positive flaring in the pre-period. Where reported, standard deviations are in parentheses. NOC ownership share is the top-owner share when the top owner is a national oil company (PDVSA, YPF, Petrobras, Ecopetrol, EP Petroecuador, Pemex), and zero otherwise. Brazil includes onshore fields only; Mexico includes all fields.

methane column as the outcome.

5 The Composition Channel

5.1 Decomposing the Per-Barrel Rise

The composition of surviving production lowered per-barrel pollution rather than raising it, ruling out the hypothesis that the per-barrel rise came from a more emissions-intensive slate of fields. Aggregate flaring intensity is the I of Equation (2), with ι_i measured as field i's flaring per barrel and s_i as its share of production. Taking the change from the pre-period (2012–2016 means) to the post-period (2022–2024 means) and splitting it into a between-field part, a within-field part, and their interaction gives

Figure 2: Evolution of flaring, production, and spending by country

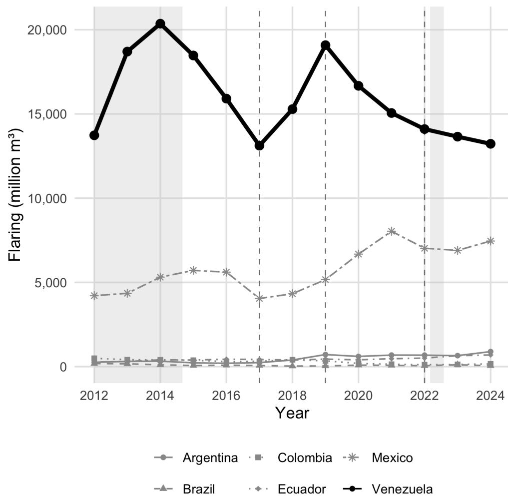

(a) Flaring (volume)

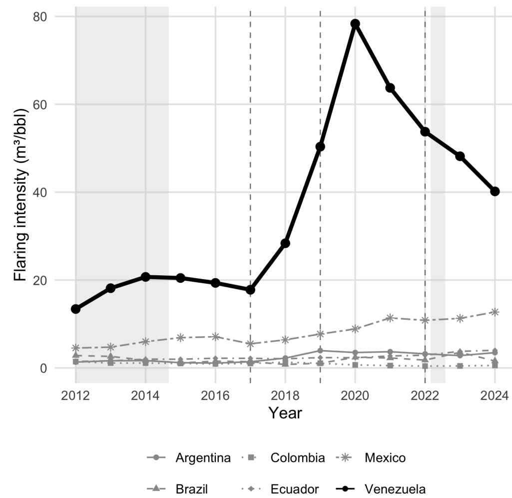

(b) Flaring per barrel

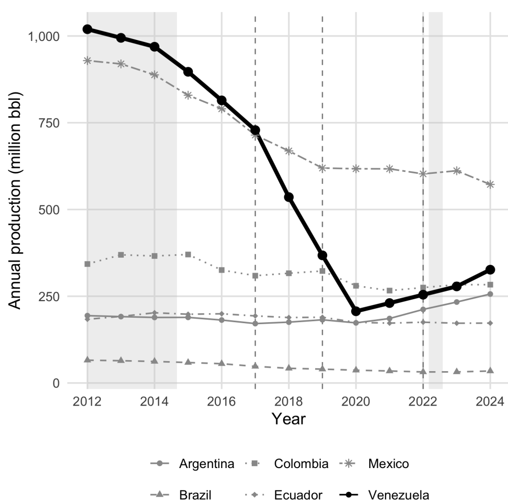

(c) Production

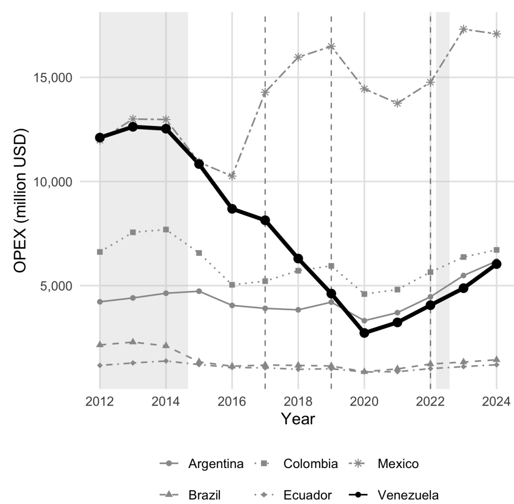

(d) Operating spending

Notes. Country-level aggregates in native units: flaring in million cubic meters, flaring per barrel in cubic meters per barrel, production in million barrels, and operating spending in million U.S. dollars. The flaring-per-barrel panel is the production-weighted mean of field intensities winsorized at the 99.5th percentile. Venezuela is the solid line; the five unsanctioned neighbors are the lighter lines. Vertical dashed lines mark the 2017, 2019, and 2022 sanctions tightenings; gray bands mark periods when Brent exceeds $100 per barrel. Flaring is World Bank VIIRS volume; production and operating spending are from Rystad UCube.

$$\underbrace{\Delta I}_{+27.8} = \underbrace{\textstyle\sum_i (\Delta s_i)\, \iota_i^{\text{pre}}}_{\text{composition} = -6.89} + \underbrace{\textstyle\sum_i s_i^{\text{pre}}\, (\Delta \iota_i)}_{\text{within-field} = +75.15} + \underbrace{\textstyle\sum_i (\Delta s_i)(\Delta \iota_i)}_{\text{interaction} = -40.5}. \tag{3}$$

Figure 3: The composition offset and the within-field rise: a counterfactual holding each field's flaring per barrel at its pre-period level

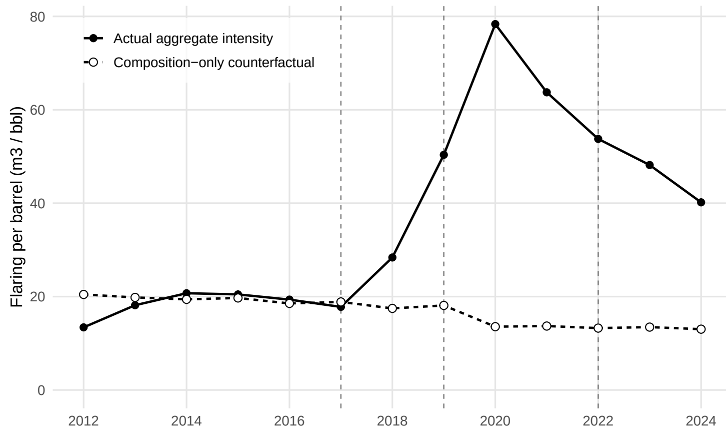

Notes. Both lines are Venezuela's production-weighted aggregate flaring intensity, in cubic meters per barrel. The dashed line with open markers is a composition-only counterfactual, $\sum_i s_{it}\, \iota_i^{\text{pre}}$, the aggregate intensity if every field kept its pre-period (2012–2016) flaring per barrel while production shares s_{it} evolved as observed. The solid line with filled markers is actual aggregate intensity, $\sum_i s_{it}\, \iota_{it}$. Vertical dashed lines mark the 2017, 2019, and 2022 sanctions tightenings. Field production is from Rystad UCube and flared volume from World Bank VIIRS under the default 15 km field-allocation rule.

The composition term holds each field's flaring per barrel at its pre-period level and moves only the production shares; it is the empirical counterpart of the operating set in the damage function, Equation (1).

Composition is an offset, not the cause. It contributes -6.89 m^3/bbl, a quarter of the total change in magnitude and with the wrong sign for an explanation: reallocation pushed aggregate intensity *down*, since the fields whose flaring per barrel rose most were the ones losing share. The rise is the within-field term, $+75.15$ gross and $+34.65$ once the interaction is included.

Figure 3 shows how small composition is. The composition-only counterfactual (dashed), holding every field at its pre-period flaring per barrel while shares evolve as observed, drifts *down* from about 20 to 13 m^3/bbl; actual intensity (solid) tracks it to 2016 and then rises about two-and-a-half-fold. The widening gap, not the drift, is the entire rise, and it is within-field, identified as strain and maintenance in Sections 6 and 7.

5.2 Which Fields Kept Producing

Which fields kept producing depends on the resource base, and a production difference-in-differences shows it. We regress $\log(1 + \text{field-level production})$ on a post-sanctions indicator interacted with field size, within Venezuela,

$$\log(1 + Y_{it}) \;=\; \mu_i \;+\; \tau_t \;+\; \theta \left(\text{Post}_t \times \text{Large}_i\right) \;+\; \varepsilon_{it},$$

where $\text{Post}_t = \mathbb{1}(t \geq 2017)$ equals one from the financial sanctions onward, Large_i marks a field above the national median in size, and μ_i, τ_t are field and year fixed effects. The fixed effects absorb Large_i and Post_t entered on their own, so the single estimated quantity is θ: how much more of its pre-sanctions output a large field kept, relative to a small one, once sanctions hit.

We measure size by oil-in-place, the resource in the ground, which geology fixes before any sanction. A large field retained 0.83 log points more production than a small one, rising to 2.95 among the heavy and extra-heavy fields (Table 2, columns 2 and 4). Past production is a weaker proxy for the same margin, since it is the outcome's own pre-period level and mean reversion pulls its gradient toward zero; measured that way the gradient keeps its sign but not its size or precision (columns 1 and 3, $+0.22$ and $+1.33$, neither significant). We therefore measure the size gradient with oil-in-place throughout.

A foreign partner preserved production alongside the resource base. A triple-difference across the six countries separates the two margins:

$$\begin{aligned}\log(1 + Y_{it}) \;=\; \mu_i \;+\; \tau_t \;+\; \theta_1 \left(\text{Post}_t \times \text{Large}_i\right) \;+\; \theta_2 \left(\text{Post}_t \times \text{PDVSA}_i\right) \\ \;+\; \theta_3 \left(\text{Post}_t \times \text{Large}_i \times \text{PDVSA}_i\right) \;+\; \varepsilon_{it},\end{aligned}$$

where PDVSA_i marks the fields the state firm ran alone and size is oil-in-place as before. The three interactions have direct interpretations. θ_1, the size gradient where PDVSA does not operate alone, is $+1.33$ and precisely estimated: across Latin America, larger fields held their output. θ_2, the extra post-sanctions fall at a small PDVSA field, is -1.41, and the corresponding fall at a large one, $\theta_2 + \theta_3$, is about -2.0: the state firm's fields lost ground at either size. The triple θ_3 itself is -0.60 and imprecise, so the data do not establish that the size gradient weakened under PDVSA operation (Table 2, column 6). They do show that resources and a

Table 2: Which fields kept producing after sanctions: the size gradient and the operator margin

	Dependent variable: log(1 + annual production)					
	(1)	(2)	(3)	(4)	(5)	(6)
Post × Large	+0.22	$+0.83^{*}$	+1.33	$+2.95^{**}$	$+1.12^{***}$	$+1.33^{***}$
	(0.44)	(0.44)	(1.02)	(1.19)	(0.16)	(0.16)
Post × PDVSA-owned					-1.21^{***}	-1.41^{***}
					(0.30)	(0.33)
× Large (triple)					-1.03^{**}	−0.60
					(0.47)	(0.47)
Sample	Ven	Ven	Ven	Ven	LATAM	LATAM
heavy/extra-heavy only			Yes	Yes		
Large	pre-prod.	OOIP	pre-prod.	OOIP	pre-prod.	OOIP
Field, year FE	Yes	Yes	Yes	Yes	Yes	Yes
Observations	2,977	2,977	806	806	21,970	21,957

Notes. Outcome is $\log(1 + \text{annual production})$ at the field-year level for fields active in the 2012–2016 pre-period. Standard errors, clustered by field, are in parentheses. "Large" is an indicator for above-country-median pre-period production (odd columns) or oil-in-place (even columns). "PDVSA-owned" is fixed at the field's pre-period ownership. Columns 1–2 use Venezuelan fields; 3–4 restrict to Rystad heavy and extra-heavy fields; 5–6 are a triple-difference on all six Latin American countries, where Post × Large is the size gradient among non-PDVSA fields and the triple is the additional gradient for PDVSA fields. $^{***}p < 0.01$, $^{**}p < 0.05$, $^{*}p < 0.10$.

foreign partner each preserved production, and that the fields with neither—small and state-run—are the ones that shut down. That is the operator margin behind the composition offset. Which partners stayed was not random, so we read the ownership contrast as corroboration; the timing evidence is the resource-size event study (Appendix Figure C.1).

5.3 Why the Survivors Have Low Flaring per Barrel

The surviving core has low flaring per barrel because of geology, not superior operating practice. Its extra-heavy crude is so biodegraded that its gas–oil ratio is essentially zero (0.001 against 0.16 for the rest), leaving almost no associated gas to flare; in levels the foreign-operated survivors flared 2.1 m^3/bbl before sanctions against 22.0 at the PDVSA-run fields, and their share of national production rose from 18 to 34 percent while PDVSA's fell from 78 to 64. Reallocating the average barrel toward them lowers aggregate intensity, which is why composition offsets part of the rise.

Operation, not geology, is the margin that kept these fields alive. The survivors were the fields a foreign partner continued funding through the sanctions: the Venezuelan joint ventures whose partner stayed held up far better than the fields PDVSA ran alone, and in the field-level survival regressions (Appendix Table C.1) such a venture retains about a log point more production than a PDVSA-run field even after oil-in-place, age, and baseline flaring are held fixed.

The institutional evidence is consistent with this interpretation. The Orinoco ventures that kept exporting were the ones that a foreign partner ran and that could blend or upgrade their crude into a marketable grade (Chevron's PetroPiar, China's CNPC at Sinovensa, which blends extra-heavy crude into the Merey export grade, and the other foreign-operated blocks of Carabobo and Junín (Chávez Alava and Vaz, 2021)), while the fields PDVSA ran alone could neither fund their upkeep nor move their crude. Resource size carries no comparable raw advantage once the depleted big-producers are set aside. Sanctions limited the state firm's ability to operate its fields, so surviving production concentrated in the foreign-operated, gas-poor Faja core, and the composition offset ultimately reflects the operator margin.

5.4 Robustness

The offset is robust to how it is measured. The between-field term stays negative across three pre/post windows and both flaring buffers (Appendix Table C.4), and it is more negative still when the composition term of Equation (3) is evaluated at post-period intensities (-47.4) or at the midpoint (-27.1); the pre-period weighting we report, at -6.89 m^3/bbl, is the smallest of the three in magnitude. The selection behind it holds when the outcome is whether a field shut down altogether rather than how much it produced, where the resource base predicts survival within Venezuela and past output does not (Appendix Table C.2); the survivors are at once low-gas Faja fields and foreign-operated joint ventures, making the offset both a crude-type and an ownership phenomenon (Appendix Table C.5); and reweighting the comparison fields onto Venezuela's covariate profile leaves the oil-in-place gradient and the PDVSA contrast intact (Appendix Table C.3). In an unreported check, two-way clustering by field and year moves the size gradient's standard error only from 0.44 to 0.45.

6 The Strain Channel

This section and Section 7 take up the within-field term of the decomposition in Equation (3), the part of the per-barrel rise that composition does not explain. Two forces drive it: strain, the gas an underfunded diluent and gas-handling chain can no longer move (this section), and maintenance, the collapse of the upkeep that holds per-barrel flaring down (Section 7).

6.1 The 2019 Break and the Departure of the Western Partners

The break in damage occurs in 2019, not at the first sanctions, and at the fields the foreign partners left (Figure 4). Flaring per barrel at the Venezuelan fields whose Western partner exited held near 5 m^3 through 2017, then climbed after the January 2019 naphtha embargo to a peak near 30 in 2020; at comparable fields elsewhere that a national oil company inherited, it stayed flat below 5.

Investment explains the timing. At the foreign-partnered fields it was cut first and deepest, to a third of its 2016 level by 2018 and a tenth by 2020, while operating spending and output held up longer. The 2017 financial sanctions cut off the capital to build and replace, but the fields ran on what they had until, by 2019, worn compressors and gathering lines could no longer be repaired, and at the limit failed outright, a 2021 pipeline explosion alone halting some 85 wells (Berg, 2021). Strain is gas the degraded infrastructure can no longer move, appearing with the lag that infrastructure takes to wear out.

The turnover concentrates production on fewer fields. Share-weighted by international partner, the Western majors' Venezuelan resource base contracts after 2017 as they exit, while the Russian partners that stayed expand and the Chinese hold flat; flaring follows, falling at the departing majors and rising at the survivors, against an unsanctioned-neighbor benchmark that moves neither way (Appendix Figures D.1 and D.2). As the majors leave, their fields pass to the remaining partners and to PDVSA, so output and its associated gas pile onto a shrinking set whose gas-handling chain is pushed past what it was built for.

The raw data show it: by 2022–2024 the number of producing Venezuelan fields

Figure 4: The 2019 break: flaring per barrel and the collapse of investment at the joint-venture fields

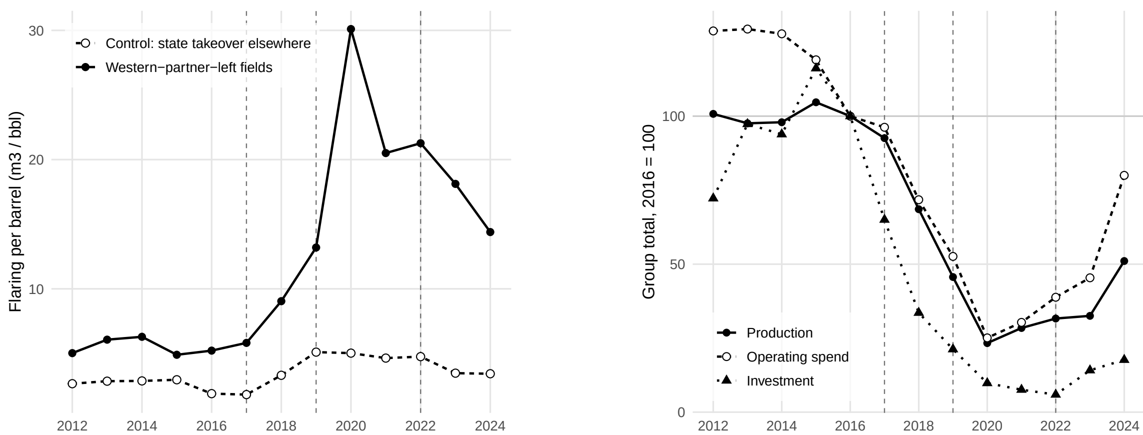

(a) Flaring per barrel

(b) Investment, operations, and output

Notes. Panel (a): group sums of flared volume over production, in cubic meters per barrel. The solid line with filled markers is the Venezuelan fields whose Western joint-venture partner exited after 2017; the dashed line with open markers is fields elsewhere in Latin America where a national oil company inherited an exiting international major. Panel (b): the Venezuelan joint-venture fields, group sums indexed to 2016 = 100, for oil production (solid), operating spending (dashed), and investment (dotted). Vertical dashed lines mark the 2017, 2019, and 2022 sanctions tightenings. Production, spending, and investment are from Rystad UCube; flared volume from World Bank VIIRS.

had fallen from 217 to 157, a 28 percent contraction against no more than 11 percent anywhere else, while the five largest fields' share of output rose from 34 to 44 percent. Argentina also concentrates over this window, but by expansion, new Vaca Muerta shale supplying four of its five largest fields; Venezuela's is by contraction, exiting fields pushing their volume onto survivors built for less. That is the strain channel in volume terms; the rest of this section identifies it from price variation.

6.2 A Price Shock From Outside Venezuela

The strain channel is venting: methane released without combustion when the diluent and gas-handling chain is financially constrained. Across Venezuela the satellite flared volume changes far less than output after 2017, ending the period near its 2012 level even as output falls by about two-thirds (Appendix Figure D.3), so the gas the failing system lost beyond the flare escaped without being burned, invisible to VIIRS but not to a methane sensor.[5] We identify this channel using the naphtha price.

Without imported diluent, Orinoco upstream operations fail within about six weeks (Grünberger, 2025). The price of that diluent is set on world markets, far from Venezuela, and cannot respond to the methane over any one Venezuelan field. When it rises, the diluent budget buys less, crude backs up in the gathering system, and gas that would otherwise move with the diluted stream escapes. For each roughly 10×10 km grid cell i and month t we observe the TROPOMI methane column $\mathrm{XCH}_{4,it}$ and estimate

$$1000 \cdot \log \mathrm{XCH}_{4,it} \;=\; \xi_i \;+\; \lambda_t \;+\; \sum_k \kappa_k \left[\log \mathrm{naphtha}_t \times \mathrm{class}_k(i)\right] \;+\; \varepsilon_{it}. \qquad (4)$$

The two fixed effects make every comparison within a cell and within a month. The cell effects ξ_i absorb each cell's own baseline methane (a wetland, a city), so the regression compares a cell only to its own average; the month effects λ_t absorb whatever is common to a month, the global trend, the seasons, the pandemic. What remains is how a cell's methane co-moves with the naphtha price, and κ_k measures that co-movement for cells of type k, against background cells far from any field or pipe. The factor of 1000 is cosmetic: coefficients are in thousandths of a log point.

The cells fall into six classes, and the design rests on the contrast among them. Four are field classes, cells within 20 km of a field: the extra-heavy Faja wellheads (κ_1), the conventional Maturín wellheads (κ_2), the Maracaibo wellheads (κ_3), and other oil-field cells (κ_4). Two are pipeline corridors, cells near the network but away from any wellhead, each assigned to the system it runs alongside: the Faja-adjacent corridor of the diluted extra-heavy stream (κ_5) and the conventional-crude corridor of the east (κ_6).

The chain of Section 3.2 predicts where methane should track the price and where it should not. It should rise along the heavy-crude corridor, where naphtha thins the crude, and at the conventional eastern wellheads, gas-rich fields with no working sink; it should stay flat at their physical counterparts outside the channel—the gas-poor Faja wellheads and the no-diluent conventional corridor. The sample is 25,545 cell-months from November 2018 to December 2024, and Table 3 reports

[5] Outside analysts describe the same failure, flared-gas volumes holding up even as oil production fell, as the sector lost the capacity to collect and reinject its gas (Berg, 2021).

every class at 10, 20, and 50 km.

The loadings κ_k of Equation (4) show a distinctive pattern, and the pipeline corridors carry it (Table 3). The heavy-crude corridor responds strongly: a one-log-point rise in the naphtha price lifts the methane column there by $+10.2$ thousandths of a log point ($p < 0.01$ at 20 km), growing with the corridor's reach from $+4.8$ at 10 to $+13.4$ at 50. The conventional-crude corridor, the corresponding pipeline-cell class nearest conventional fields, does not move at any radius ($+1.3$, not significant). Two sets of pipeline cells are separated by their connection to the Faja diluent system, and only the Faja-adjacent one responds. The pattern is a transport channel rather than a point source or mislocated wellhead gas: the responding cells sit a median of 66 km from any field, and the corridor loading survives nearly unchanged ($+9.9$) when every corridor cell within 40 km of a wellhead is dropped.

The oil-field cells confirm the channel and locate a second one. The extra-heavy Faja wellheads, sitting on crude with almost no associated gas, do not respond ($+1.7$); the conventional Maturín wellheads do carry a smaller positive signal ($+3.4$, $p < 0.10$, stable across radii). That is the diluent substitution of Section 3.2: a high price for the imported diluent draws Maturín light crude toward the export blend and strains the fields that supply it, and their associated gas, with the El Furrial reinjection idle, escapes because nothing is in place to hold it. A field already losing its gas for lack of a sink loses more of it the moment it is strained. The Maracaibo wellheads carry a *negative* loading (-5.35, $p < 0.01$), and we do not read it as a diluent-chain response. The methane over those cells is dominated by the Lake Maracaibo complex, which emits on the order of 1.2 Mt a year, about a sixth of Venezuela's total, roughly half of it from the lake's aging oil infrastructure and the rest from other sources (Nathan et al., 2024); none of it runs on naphtha, since Maracaibo crude moves without diluent (Section 3.2). The class is reported for completeness, and the strain reading rests on the corridor and conventional-wellhead contrasts.[6]

The response is concentrated in the current month and the first lag and then reverses (Appendix Table D.1). Venezuela does not buy diluent on the spot market month to month, so the price affects operations with a short delay; a price spike

[6] Excluding the Maracaibo cells leaves the other classes essentially unchanged (Appendix Table D.6): at the 20 km radius the heavy-crude corridor loading moves from $+10.2$ to $+9.8$ and the Maturín loading from $+3.4$ to $+3.3$, each retaining its significance, while the Faja wellheads and the conventional corridor remain small and insignificant.

Table 3: Strain on the diluent supply chain and the methane column, by cell type

	Coefficient on $\log(\mathrm{XCH_4})$ ($\times 10^3$)		
Cell type	10 km	20 km	50 km
Oil-field cells (within the radius of a wellhead)			
Cells near the Faja extra-heavy fields	$+0.43$	$+1.74$	$+0.96$
	(2.58) [14]	(1.68) [41]	(1.39) [93]
Cells near the conventional fields (Maturín)	$+3.05^{*}$	$+3.41^{*}$	$+3.22^{*}$
	(1.71) [20]	(1.75) [26]	(1.76) [29]
Cells near the Maracaibo fields	-10.37^{***}	-5.35^{***}	-1.92^{*}
	(1.72) [15]	(1.93) [51]	(1.06) [133]
Other Venezuelan fields	$+0.86$	-1.20	$+0.71$
	(1.90) [13]	(0.79) [32]	(0.68) [116]
Pipeline-corridor cells (near a line, away from any wellhead)			
Heavy-crude pipeline corridor	$+4.80$	$+10.15^{***}$	$+13.44^{***}$
	(3.35) [29]	(2.90) [50]	(2.64) [66]
Conventional-crude corridor	$+1.80$	$+1.33$	$+1.15$
	(1.46) [77]	(1.05) [123]	(0.88) [190]
Cell fixed effects	Yes	Yes	Yes
Year-month fixed effects	Yes	Yes	Yes
Cell-months	25,545	25,545	25,545
Cells	1,280	1,280	1,280

Notes. Each column is a single regression of $\log(\mathrm{XCH_4})$, multiplied by 10^3, on the global naphtha price interacted with an indicator for cells of that type, estimated over Venezuelan satellite grid cells for 2018–2024; background cells are the omitted reference. Standard errors, clustered by cell, are in parentheses. Bracketed figures are the number of cells in each class at that radius. Appendix B details the construction of the cell classes. $^{***}p < 0.01$, $^{**}p < 0.05$, $^{*}p < 0.10$.

defers purchases and lifts venting now, and the catch-up restocking once the price falls back lowers venting a few months later, so the coefficients on the later lags are negative. A future-price placebo is null, so the methane does not anticipate the move.

6.3 Identification and Cross-Country Evidence

The design's strength is cross-sectional. Naphtha and Brent move almost as one over our window (correlation 0.96), so the price level alone cannot separate the cost of diluent from the global oil cycle. The cross-class contrasts can: a common oil-price confounder would have to lift methane along one pipeline-corridor class but not the physically comparable class beside it, and not at the extra-heavy wellheads, which is not what an aggregate price shock does.

A cross-country comparison shows the pattern is specific to sanctioned Venezuela. Because flaring turns methane into carbon dioxide, one might worry the satellite signal tracks where flaring fell rather than where venting rose. The heavy-oil basins of the unsanctioned neighbors say otherwise (Appendix Table D.2): relative to wellhead cells in no heavy-oil basin, Venezuela's Orinoco Belt trends up (+1.30 per year, $p < 0.01$ at 20 km), while Mexico's Maya (−2.51) and Colombia's Llanos (−0.81) trend down; Ecuador's Oriente rises (+1.51), but on a profile of steady expansion rather than a sanctions shock. Appendix Table D.3 formalizes the comparison in a triple difference on the pooled six-country panel. We regress the methane column on a linear time trend interacted with whether a cell is in Venezuela and whether it sits near a pipeline,

$$\log \mathrm{XCH}_{4,it} = \xi_i + \tau_t + \psi_0 \, (t \times \mathrm{Venezuela}_i) + \psi_2 \, (t \times \mathrm{NearPipe}_i) \\ + \psi_1 \, (t \times \mathrm{NearPipe}_i \times \mathrm{Venezuela}_i) + \varepsilon_{it},$$

with cell and year-month fixed effects. Venezuela's trend away from pipelines is *negative* ($\psi_0 = -0.89$ per year), so the rise is not country-wide; the near-pipeline trend in the comparison countries is also negative ($\psi_2 = -0.29$), so a pipeline on its own does not lift methane. The extra trend that a pipeline carries specifically in Venezuela is positive at every radius ($\psi_1 = +0.88$ per year, $p < 0.01$); estimated separately within Venezuela and within the comparison countries, the near-pipeline trend is +0.67 inside Venezuela and −0.28 outside (Appendix Table D.3, Panel A). The methane rise is confined to Venezuela's pipeline corridors.

The corridor result is stable across the choices that could drive it. It holds under two-way clustering, a cell-specific seasonal fixed effect, a region-by-year-month fixed effect, and dropping the pandemic years 2020–2021 (Appendix Table D.4); the conventional-corridor placebo stays small and insignificant throughout, except under the cell-seasonal fixed effect, where it becomes significant at a third of the heavy-corridor loading. A spatial placebo redraws the corridor at random 999 times, and the observed loading lies beyond every draw (Appendix Figure D.4, permutation $p = 0.001$); it also survives varying the radius and dropping cells within 30 to 50 km of any wellhead (Appendix Table D.5).

7 The Maintenance Channel

Section 6 traced gas escaping where the diluent chain was starved; maintenance is the other within-field force, the collapse of the routine upkeep that, when funded, lowers the gas each barrel flares. That upkeep had been eroding at PDVSA before sanctions, and the sanctions deepened the erosion by cutting the imported parts and foreign service firms it depends on (Gugarats, 2024).[7] The channel is the hardest of the three to identify, because spending and output move together; the sanctions regime itself supplies the experiment. In November 2022 G.L. 41 let Chevron, and only Chevron, resume operating its four Venezuelan joint ventures, authorizing their production and their *maintenance, repair, and servicing* while barring any payment of taxes, royalties, or dividends to the state (Congressional Research Service, 2024; Gilroy et al., 2022). For one operator it lifted the input constraint—spare parts, expertise, and financing for upkeep—while leaving the revenue squeeze on the regime untouched; by 2025 the ventures it covered accounted for between a quarter and a third of national output (Hajdari, 2025), and no other operator received the same relief. It shifts maintenance at a handful of fields, on a known date, for reasons unrelated to those fields' pollution.[8]

7.1 A Triple-Difference for the Maintenance Elasticity

To separate maintenance from strain we estimate the elasticity of flaring to the maintenance budget m_i of Equation (1), proxied at the field-year level by per-barrel operating expenditure, $m_{it} = \log(1 + \mathrm{OPEX}_{it}/\mathrm{prod}_{it})$.[9] The obstacle is that spending and flaring move together for reasons unrelated to upkeep: a field

[7] For instance, Berg (2021) reports technical staff shed in the 2000s, plant left uninspected, and one Punta Cardón facility unchecked since 2016 despite a standing maintenance order.

[8] G.L. 44 of October 2023 briefly eased sanctions on the whole sector before its 2024 reimposition. It falls at the end of our window and, if anything, works in favor of a conservative estimate: any relief at the comparison fields makes the controls behave more like the treated Chevron fields, narrows the treated–control gap, and pulls η_5 toward zero.

[9] Flaring allocates precisely to fields: a flare is a bright point source, assignable to the field beneath it. The methane column does not. We therefore measure the license effect with flaring, and use methane only for the strain price response across cell classes (Section 6).

pumping hard spends more and flares more, so a naive regression confounds the maintenance margin with the scale of operations.

The license breaks the confound. It raised m_{it} at the Chevron fields, on a known date, for reasons external to those fields' own output decisions, so the change in the spending–flaring relationship there after the license is the identifying contrast. We recover it from a saturated triple-difference of flaring volume on per-barrel spending:

$$\begin{aligned}\log(1+F_{it}) \;=\; \eta_1\, m_{it} \;+\; \eta_2\left(m_{it}\times \text{Post2017}_t\right) \;+\; \eta_3\left(m_{it}\times \text{Post2022}_t\right) \\ +\; \eta_4\left(m_{it}\times \text{Chevron}_i\right) \;+\; \eta_5\left(m_{it}\times \text{Post2022}_t\times \text{Chevron}_i\right) \\ +\; \delta\left(\text{Post2022}_t\times \text{Chevron}_i\right) \;+\; \mu_i \;+\; \tau_t \;+\; u_{it}.\end{aligned} \tag{5}$$

Here F_{it} is flaring volume; Post2017_t and Post2022_t mark the financial-sanctions and license windows, with $\text{Post2022}_t = 1$ in 2023–2024, the first full post-license years; and Chevron_i marks the treated fields. The field and year effects μ_i, τ_t absorb Chevron_i, Post2017_t, and Post2022_t entered on their own, along with every fixed field difference and every shock common to a year.

The remaining terms are the slopes on spending, read one at a time. η_1 is the baseline spending–flaring slope at an untreated field before sanctions; η_2 and η_3 let it shift in the two sanctions windows, common to all fields; η_4 lets it differ at the Chevron fields throughout, absorbing any fixed peculiarity of their technology; and δ is a level shift in Chevron flaring after the license, the part that does not run through spending. The coefficient of interest is the triple η_5: the change, at the treated fields and after the license only, in how an extra unit of per-barrel spending maps into flaring. Because the outcome is log flaring *volume*, the specification does not fully hold production scale fixed, so η_5 is a conditional slope after those absorptions, not the net license effect.

Table 4 estimates Equation (5) under three fixed-effect structures. The triple η_5 is stable and negative, at about -0.54 in the first two columns and -0.63 in the third. The inference is deliberately conservative. The two-way clustering common in applied work would put every column past the five percent level, but with only three Chevron fields[10] and six post-2022 treated field-years it overstates

[10] G.L. 41 covered Chevron's four Venezuelan joint ventures. The fourth, PetroIndependiente, operates the offshore LL-652 field in Lake Maracaibo; since our field-level samples include onshore

precision; standard errors corrected for the few treated clusters, the CR2 bias-reduced estimator with Satterthwaite degrees of freedom (Pustejovsky and Tipton, 2018; Imbens and Kolesár, 2016), put the baseline at $p = 0.09$ and the other columns just above 0.10 (exact values in the table). In unreported checks, a restricted field wild-cluster bootstrap and a placebo that reassigns the three treated-field labels put the baseline at $p = 0.121$ and $p = 0.127$ (999 draws each), the bootstrap itself conservative with few treated clusters (MacKinnon and Webb, 2018). We treat it as a suggestive maintenance slope, not a precisely estimated effect.[11]

The maintenance channel predicts a negative η_5: where the license restored the upkeep budget, an added unit of per-barrel spending buys a larger cut in flaring than the same spending elsewhere, the marginal dollar going to leak repair and gas capture rather than to throughput. The level term δ is large and positive ($+1.88$), and it carries the key caveat: the license also restarted production, roughly doubling the treated fields' output from its 2021 trough, so their flaring rose in absolute terms as the wells came back. We therefore read η_5 as a conditional association: within this specification, a one-percent rise in maintenance spending per barrel is associated with about 0.54 percent lower flaring volume.

7.2 The First Stage

The triple-difference requires the license to have moved maintenance spending at the treated fields. Figure 5 shows that it did, plotting the yearly gap in operating spending between the Chevron fields and other Venezuelan producers, with 2021 as the reference: flat through 2021, then rising after November 2022 by about 0.38 log points, some 45 percent, over 2022–2024. The flat pre-license path ties the break to the license rather than to a pre-existing trend, and the rise reflected real activity, not accounting, with Chevron resuming drilling at its existing Carabobo blocks and undertaking no new development (Onsat, 2024). This spending rise, external to the fields' own output decisions, identifies η_5.

fields only, three Chevron fields enter the estimation.

[11] In an unreported robustness check, excluding the partial 2022 transition year, when the license took effect only in November, leaves the elasticity at -0.634 (standard error 0.123, significant at ten percent), so the magnitude is not an artifact of the changeover.

Table 4: Maintenance channel: per-barrel OPEX and flaring volume

	Flaring volume $\log(1+F_{it})$		
	(1)	(2)	(3)
Panel A. Triple-difference estimates			
$\log(1+\text{OPEX/prod})$ (η_1)	-0.0511^{***}	-0.0513^{***}	-0.0528^{***}
	(0.0172)	(0.0171)	(0.0177)
$\times$ Post2017 (η_2)	$+0.0617^{***}$	$+0.0581^{***}$	$+0.0633^{***}$
	(0.0187)	(0.0191)	(0.0207)
$\times$ Post2022 (η_3)	-0.0183	-0.0159	-0.0108
	(0.0150)	(0.0153)	(0.0162)
$\times$ Chevron (η_4)	-0.1686	-0.2797	-0.1228
	(2.9029)	(2.9206)	(2.9224)
$\times$ Post2022 $\times$ Chevron (η_5)	-0.5441^{*}	-0.5383	-0.6308
	(0.0998)	(0.1087)	(0.1301)
Post2022 $\times$ Chevron (δ)	+1.8764	+1.8901	$+2.0956^{*}$
	(0.3985)	(0.3810)	(0.3189)
Field FE	Yes	Yes	Yes
Year FE	Yes	Yes	Yes
Heavy share $\times$ Year	No	Yes	No
Orinoco-East $\times$ Year	No	No	Yes
Observations	2,309	2,309	2,309
Panel B. Exact p-values for the maintenance elasticity η_5			
CR2/Satterthwaite	0.092	0.103	0.101

Notes. Saturated triple-difference test of the maintenance channel. Dependent variable: $\log(1+\text{flaring volume in million m}^3)$ at the field-year level; sample: Venezuelan onshore field-years with positive production, 2012–2024; Post2022 equals one in 2023–2024, the first full post-license years. Standard errors, clustered by field, are in parentheses. Panel B reports the exact p-value for η_5 in each column. $^{***}p < 0.01$, $^{**}p < 0.05$, $^{*}p < 0.10$.

8 Discussion

The three channels are identified. This section adds them up, values them at the social cost of carbon and methane, develops the externality that makes maintenance a policy lever, and draws out the implications for sanctions design and the investment gap.

8.1 Adding Up the Per-Barrel Damage Rise

How far does actual damage depart from the proportional-decline benchmark of Section 2? Let D_{pre} be total flaring damage in the pre-sanctions baseline and

Figure 5: G.L. 41 at the Chevron fields: the first stage on maintenance spending

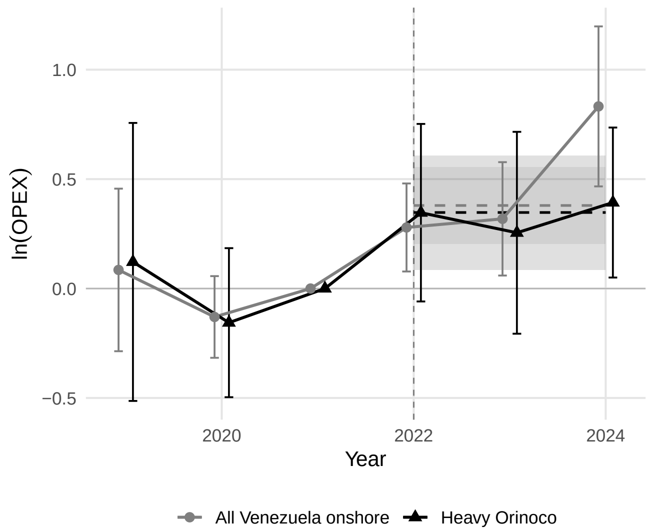

Notes. Event-study coefficients for log operating spending at the Chevron-operated fields relative to other Venezuelan producers, by year, with 2021, the year before the license, as the omitted reference year; the dashed line marks the pooled 2022–2024 difference-in-differences with its 95% band. Two comparison samples: all Venezuelan onshore producers (gray circles) and heavy-Orinoco producers only (black triangles). The regressions use Venezuelan onshore field-years with positive operating spending over 2017–2024 and control for field and year fixed effects; plotted coefficients are shown for 2019–2024, with standard errors clustered by field. Operating spending and production are from Rystad UCube.

D_{post} the 2022–2024 average. Output fell by $\rho \equiv 1 - Q_{\text{post}}/Q_{\text{pre}} \approx 0.7$. Under the benchmark, damage falls one-for-one with output,

$$D^{\text{ctf}}_{\text{post}} \;\equiv\; (1-\rho)\, D_{\text{pre}} \;=\; \tfrac{Q_{\text{post}}}{Q_{\text{pre}}}\, D_{\text{pre}}, \tag{6}$$

holding per-barrel intensity, the operating set, and proximity to capacity at their pre-sanctions values. The departure from the benchmark is the ratio of actual to counterfactual damage, $R \equiv D_{\text{post}}/D^{\text{ctf}}_{\text{post}} = (D_{\text{post}}/D_{\text{pre}}) \cdot (Q_{\text{pre}}/Q_{\text{post}})$, which is exactly the ratio of post- to pre-sanctions per-barrel intensity. In Venezuela that ratio is $R \approx 2.4$: production-weighted flaring intensity rose from 20.3 to 48.1 m^3/bbl while output fell by about two-thirds, so total flaring damage declined by only about a fifth and per-barrel damage more than doubled.

The headline result does not depend on how flaring damage is measured. Across the 10 and 15 km allocation buffers and the alternative pre/post windows, the within-field rise stays between about $+30$ and $+38$ m^3/bbl and the composition offset between -5 and -7 (Appendix Table C.4). The rest of this section decomposes this rise into the three margins.

The shift-share of Equation (3) splits $R-1$ into the channels. Figure 6 draws it. Composition is an offset: it is the between-field term of Equation (3), $\sum_i \Delta s_i \, \iota_i^{\text{pre}} = -6.89$ m^3/bbl, which holds every field's pre-sanctions flaring per barrel fixed and moves only the production shares, so it measures the reallocation alone. Because the fields that kept producing are the lower-intensity, foreign-operated survivors, the reallocation lowers aggregate intensity. The two within-field forces more than offset it. Strain (the gas an underfunded diluent and gas-handling chain can no longer move) adds 23.5, the largest single channel; the collapse of routine maintenance adds 11.2. The three sum to the observed rise.[12]

The split between composition and the within-field rise is exact; the split between strain and maintenance is set by the paper's one causal maintenance estimate. The shift-share separates the producing mix from what happens inside surviving fields, but it cannot by itself distinguish vented gas from worn-out equipment, because both raise per-barrel flaring at a field held fixed. We apportion the within-field rise with the Chevron elasticity: deferred upkeep accounts for about a third of it, leaving two-thirds to strain. The decomposition also rejects the most immediate reading of the aggregate rise. A more-than-doubling of pollution per barrel is consistent with Venezuela's highest-intensity fields coming to dominate the mix, but the shift-share shows the reverse. The producing mix moved toward lower-intensity fields, and the rise happened entirely inside the fields that survived, over and above the offsetting shift in the mix.

8.2 The Climate Cost

Flaring is the smaller part of the climate cost. Venezuela flared roughly 13.7 bn m^3 of gas a year over 2022–2024; by 2025 that was about one in every twelve m^3 of

[12]To separate the within-field effect into maintenance and strain, note the within-field terms of Equation (3) sum to $75.15 - 40.50 = 34.65$ m^3/bbl. Two estimates then pin down the maintenance share. The elasticity $\eta_5 = -0.544$ of Equation (5) (Table 4, column 1) gives how far flaring falls when upkeep rises, and $\beta^{\text{OPEX}} = -0.514$ (Appendix Table B.1) gives how far sanctions cut operating spending. Their product is the log rise in flaring that the lost upkeep accounts for, so the maintenance share of 34.65 is $\phi \equiv \exp\left(\eta_5 \, \beta^{\text{OPEX}}\right) - 1 = 0.323$. Maintenance therefore contributes $0.323 \times 34.65 = 11.2$ m^3/bbl and strain the residual, $(1 - 0.323) \times 34.65 = 23.5$.

Figure 6: The per-barrel flaring-intensity rise decomposed into composition, strain, and maintenance

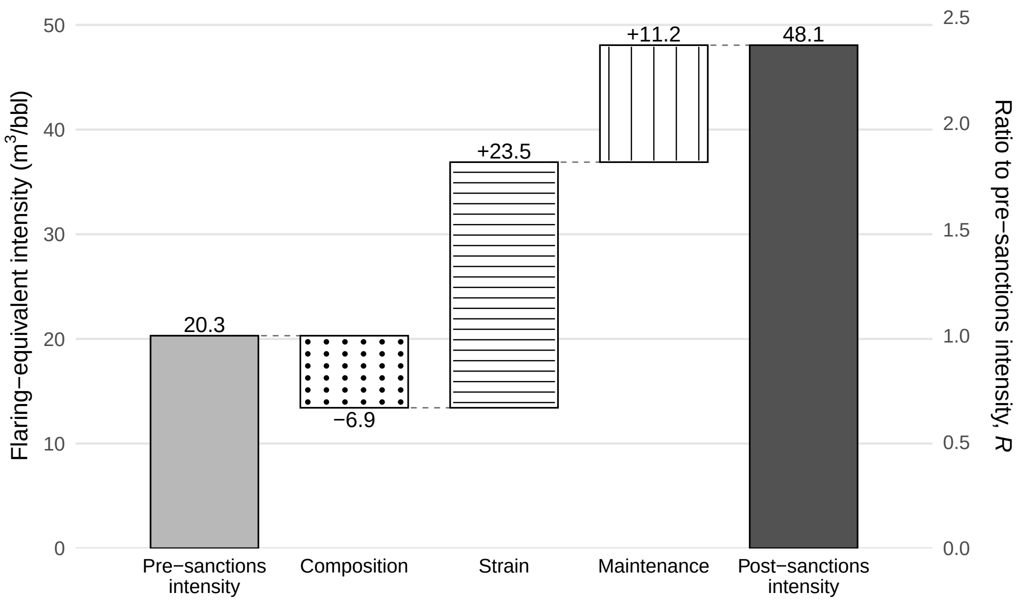

Notes. Production-weighted mean flaring-equivalent intensity of Venezuelan onshore fields, pre-sanctions (2012–2016) versus 2022–2024, in cubic meters per barrel. Composition is the shift-share term $\sum_i \Delta s_i \, \iota_i^{\text{pre}}$; the within-field rise $\sum_i s_i^{\text{pre}} \Delta\iota_i$, with the interaction included, is split into strain and maintenance in the ratio 68:32, the share apportioned to restored upkeep through the Chevron maintenance elasticity of Section 7. Field production is from Rystad UCube and flared volume from World Bank VIIRS.

gas flared on Earth, from a country producing roughly one percent of the world's oil (World Bank, 2026). Burned, that gas releases on the order of 27 Mt of carbon dioxide a year, about \$5 bn of climate damage at the EPA's central social cost of carbon of \$190 per metric ton (U.S. Environmental Protection Agency, 2023). The proportional-decline benchmark (6), which takes the output collapse as given, splits this bill: at pre-sanctions intensity (20.3 against today's 48.1 m^3/bbl) today's output would do about \$2 bn of flaring damage a year, so roughly \$3 bn of the \$5 bn is excess, a failure of flaring to fall with output rather than a rise in flaring, whose total fell.

The gas vented rather than burned does more damage and is not detected by the flaring satellite: methane warms the climate many times more, ton for ton, than the carbon dioxide from a flare. Venezuela's oil and gas operations vent on the order of 3.6 Mt of methane a year, an emissions intensity six times the global average and the largest source in South America (International Energy Agency, 2025; Kennedy, 2026); at the EPA's social cost of methane of $1,600 per metric ton (U.S. Environmental Protection Agency, 2023), that venting does roughly $6 bn of climate damage a year, above the flaring cost, and larger still once methane's stronger near-term warming is weighted. The $5 bn of flaring damage on 286 mn barrels a year is about eighteen dollars a barrel, and the full climate cost (flaring and venting together) comes to roughly forty, a cost of the same order as the barrel's sale price.

This venting cost ($6 bn) is a level, not a sanctions increment. The mechanism ties the venting to sanctions: the conventional-field methane column responds to the naphtha price where the strain mechanism predicts (the Maturín loading of Table 3), pointing to the underfunded diluent chain rather than to geology or weather. The mechanism does not quantify the increment: a price with no trend across the sample identifies venting from month-to-month variation and yields no cumulative tonnage, and turning the satellite response into a field-level flux would need an atmospheric inversion, the methane being measured on 10 km cells while plumes drift tens of kilometers on the wind (Lauvaux et al., 2022). Nor can the satellite record supply the counterfactual: TROPOMI observations begin in 2018, after sanctions. Within their window the collapse is visible: Lake Maracaibo output fell by 60 percent over 2018–2020 with no significant decline in methane, and the share of produced energy lost as methane roughly doubled, from 11 to 23 percent, against 1–4 percent in producing regions elsewhere (Nathan et al., 2024).

The benchmark still yields a bound. The same rule (6), applied to venting rather than flaring, scales the pre-sanctions level down by the fall in output: production fell to a third, so counterfactual venting is a third of whatever Venezuela vented before sanctions. That level is unmeasured, but one assumption caps it: the sector at three times today's output, its gas handling still running, vented no more in absolute terms than the 3.6 Mt it vents today. The counterfactual is then at most 1.2 Mt, the excess at least 2.4 Mt, and at least two-thirds of the $6 bn, some $4 bn a year, sits above the benchmark, an inequality under that one assumption rather than an estimate.

Beyond that bound we apportion no further: the $6 bn prices what Venezuela's operations vent in a year, whether the underlying neglect predates the sanctions or not. Adding the measured flaring excess and the bounded venting excess puts the sanctions-attributable climate damage at roughly $7 bn of the $11 bn a year, more than two-fifths of the \$16 bn a year in oil revenue the sanctions cost Venezuela (Rodríguez, 2022).

8.3 The Uninternalized Externality of Maintenance

The maintenance margin is a policy lever because its climate benefit is an externality. Operating expenditure m_i lowers a field's per-barrel intensity, $\alpha_i'(m_i) < 0$: spending on leak repair, compressor parts, and gas capture suppresses the flaring and venting that the field would otherwise emit. That suppressed pollution—carbon dioxide and, above all, methane—is a global externality the operator does not capture: its private return to upkeep is the oil it keeps flowing and the equipment it keeps from failing, while the climate damage avoided accrues to everyone else. The social return to maintenance therefore exceeds the private, as with investment in innovation once spillovers are counted (Bloom et al., 2013), and upkeep is under-provided even absent sanctions.

The operator chooses m_i to set the marginal private value of spending to zero; the planner adds the avoided climate damage, $-\,\mathrm{SC}\cdot\alpha_i'(m_i)\,q_i > 0$, where SC is the social cost of the carbon and methane the spending suppresses, and so picks a higher budget. Sanctions that cut m_i push it further below the social optimum, creating an uninternalized external cost that the output statistics do not record.

The Chevron license provides a suggestive estimate of the wedge: the maintenance elasticity of Section 7, $\eta_5 = -0.54$. Read as an abatement elasticity, it is a lower bound: the regressor is total operating expenditure per barrel, not dedicated abatement spending, so its variation is a noisy proxy for the upkeep that suppresses flaring, and η_5 is attenuated toward zero. The elasticity on abatement spending alone, the object that structural models of the abatement technology recover (Shapiro and Walker, 2018), would be larger.[13]

The decomposition quantifies what restoring upkeep more widely could deliver: the maintenance slice of the per-barrel rise (11.2 m^3/bbl on roughly 286 mn barrels a year) is about 3.2 bn m^3 of avoidable flaring a year, some 6.4 Mt of carbon dioxide, or \$1.2 bn of climate damage at the EPA social cost, roughly a quarter of the flaring cost, before counting any venting.

[13] Duflo et al. (2018) study this margin directly: the Indian plants they study cut pollution by running and maintaining existing abatement equipment when regulatory pressure raises the return to it.

8.4 Generalization to Other Sanctioned Producers

The logic we propose is general: when sanctions cut output while sparing, or even concentrating, high-emissions infrastructure, per-barrel emissions rise, and any large sanctions-driven reallocation should show the same three margins. Iran after 2018 is the natural case. It is a major oil-and-gas methane emitter; sanctions have cut its output, surviving production has concentrated on a handful of large fields, and the imported inputs that hold leaks down have been restricted (International Energy Agency, 2025; Fernández-Villaverde et al., 2025). In the flaring tracker, Iranian flared volumes against EIA output imply flaring per barrel roughly a third higher after 2018 than before (World Bank, 2026). We do not run a field-level decomposition, which the opacity of post-2018 Iranian data would not support; we offer the three-channel structure as a generalization grounded in the mechanism, not as new estimates. The measurement template—flaring from VIIRS, methane from TROPOMI—does generalize: it needs no cooperation from the sanctioned producer and can be applied wherever production-side data are sparse.

8.5 Separating Financial From Technical Squeeze

The lever suggested by the results is to separate two restrictions that comprehensive sanctions bundle together but need not move together: the denial of revenue to the government, and the denial to its fields of the inputs (spare parts, expertise, diluent) that hold pollution per barrel down. The first is the geopolitical objective. The second is an environmental side effect with no geopolitical content, and the Chevron license shows the two can be separated in practice: it restored the technical inputs while the revenue ban stayed in place.

Call the instrument an *environmental carve-out*: a license for the inputs of lower-emissions operation (spare parts, service contractors, gas-capture and reinjection equipment), granted while output and revenue stay constrained. Sanctions regimes already carve out food and medicine; this is the same architecture applied to the inputs of pollution control. In the terms of the episode we study, the carve-out is G.L. 41 without its production clause: the maintenance, repair, and servicing authorities, and the diluent purchases that upkeep requires, with the authorities to produce and lift left out. The Chevron license itself was not that instrument. It bundled upkeep with a production restart, and at its fields the restart dominated, so flaring rose even as the upkeep margin improved. The design lesson is to unbundle the two and license maintenance rather than barrels.

Two design questions follow. The first is leakage: parts and contractors are fungible, and inputs licensed for upkeep can end up raising output instead, as the bundled Chevron license did by design; the answer is a narrow licensed list (compressor parts, leak repair, gas capture, reinjection) kept far from drilling and lifting services. The second is verification, and it needs no cooperation from the sanctioned state, because the compliance record is the satellite record this paper is built on. A flare is visible from orbit at the field level and the methane column at the 10 km cell, so the sanctioning authority can condition the license's renewal on observed flaring at the licensed fields rather than on the operator's or the regime's reporting. The externality of Section 8.3 provides the instrument's rationale, the maintenance elasticity its magnitude; because the revenue ban stays in place, its geopolitical cost is zero.

This lever is supply-side, and it differs from the demand-side instruments that dominate sanctions practice. A price cap works by making the highest-cost barrels the least profitable to lift; it retires high-emissions capacity where the high-emissions fields are also the expensive ones. In Venezuela the cost ordering does not line up that way. The surviving Faja core is cheap to keep pumping once diluent and upkeep are in place, so a cap would not selectively retire the high-emissions capacity, and the channel that drives the damage (inputs denied to fields that go on producing) is one that a demand-side cap does not reach. The two instruments are therefore complements rather than substitutes: one squeezes the regime's revenue, the other removes the environmental side effect. The right mix depends on whether the high-emissions capacity is expensive to run, in which case a cap retires it, or cheap to keep running, in which case licensing its upkeep cuts the per-barrel damage.

8.6 Outlook: The Investment Gap and Its Return

The deterioration this paper measures is an investment gap: the gas is vented for lack of capital and equipment, not geology. Rebuilding the gas side that sanctions underfunded—the gathering and processing plant, the diluent pipelines, the reinjection compressors, and the steam generation that heavy-oil recovery runs on (Incorrys, 2026)—would cost tens of billions that our estimates do not price. That capital must come from foreign operators, held off by the expropriation risk that a sovereign cannot credibly commit away (Fioretti et al., 2026b), while the constrained state firm cannot fund it; the venting reflects a financial constraint. Our estimates can, however, bound the return.

The climate damage that the gap causes is the social return to closing it. For as long as the gas-handling system stays broken, Venezuela does about $5 bn of climate damage a year by flaring and on the order of $6 bn by venting (Section 8.2); that cost recurs every year the gap is open, so the present value of closing it is a multiple of the annual figure. The gas now flared and vented is also a resource, not only a pollutant: captured, it is the fuel that the steam generation and reinjection of heavy-oil recovery require (Incorrys, 2026; Berg, 2021), so the capital that closes the gap earns a production return and a climate return at once. Both returns remain large while the gap stays open—the externality of Section 8.3 at the scale of the whole gas system.

The license behind these estimates has since been withdrawn: in early 2025 the United States reversed G.L. 41 and wound Chevron's operations down by 27 May (U.S. Department of the Treasury, Office of Foreign Assets Control, 2025). In that year flared volume at the Chevron fields rose by roughly half while it eased at comparable heavy-Orinoco fields, a pattern consistent with the mechanism we document. Our production and operating data from Rystad end in 2024, however, so this 2025 flaring cannot yet be turned into a per-barrel rate or a test of the channel.

9 Conclusion

Sanctions cut Venezuela's oil output by two-thirds. Yet for every barrel the country still produced, the gas flared rose by about two and a half times. This was not because dirtier fields took over the mix: the fields that kept producing were, if anything, cleaner, and the extra pollution came from inside them. Sanctions cut off the imports these fields run on: the diluent that lets heavy crude flow, spare parts, and investment. Their gas-handling equipment was pushed past its limits and its upkeep deferred, so more of the gas that comes up with the oil escaped instead of being captured, and the share of the energy produced going to waste grew as the industry shrank.

The climate cost of this deterioration is large and mostly absent from a debate that measures sanctions by their effect on production and revenue. Burning and releasing the gas causes on the order of $11 bn of climate damage a year, about forty dollars for every barrel Venezuela still produces, and we attribute roughly $7 bn of that damage to the sanctions. Part of this cost is avoidable by policy design. The inputs that hold pollution down—spare parts, servicing, and diluent—can be licensed separately from the oil revenue the sanctions are meant to deny. The 2022 Chevron license showed the separation is practicable: it restored upkeep at a handful of fields while the ban on payments to the government remained in place. A license written for maintenance rather than for output would keep the financial pressure on the regime while avoiding the collateral climate damage, in Venezuela and elsewhere.

Closing the investment gap permanently is a larger task. Rebuilding the country's decayed gas infrastructure would cost tens of billions, capital that only foreign firms can supply and that sanctions and the fear of expropriation now hold back. But the gas going to waste is both a fuel the industry itself needs and a recurring source of climate damage, so the return to fixing it is large, in recovered fuel and in avoided emissions alike. That return does not enter a sanctions calculus that counts only output and revenue.

References

AFESORGBOR, S. K. (2019): "The Impact of Economic Sanctions on International Trade: How Do Threatened Sanctions Compare with Imposed Sanctions?" *European Journal of Political Economy*, 56, 11–26.

AGERTON, M., B. GILBERT, AND G. B. UPTON, JR. (2023): "The Economics of Natural Gas Flaring and Methane Emissions in US Shale: An Agenda for Research and Policy," *Review of Environmental Economics and Policy*, 17, 251–273.

ALVAREZ, J. A., M. ARENA, A. BROUSSEAU, H. FARUQEE, E. W. FERNANDEZ CORUGEDO, J. GUAJARDO, G. PERAZA, AND J. YEPEZ (2022): "Regional Spillovers from the Venezuelan Crisis: Migration Flows and Their Impact on Latin America and the Caribbean," Departmental Paper 2022/019, International Monetary Fund, Washington, DC.

ASKER, J., A. COLLARD-WEXLER, C. DE CANNIERE, J. DE LOECKER, AND C. R. KNITTEL (2024): "Two Wrongs Can Sometimes Make a Right: The Environmental

Benefits of Market Power in Oil," Working Paper 33115, National Bureau of Economic Research.

ASKER, J., A. COLLARD-WEXLER, AND J. DE LOECKER (2014): "Dynamic Inputs and Resource (Mis)Allocation," *Journal of Political Economy*, 122, 1013–1063.

BAHAR, D., S. BUSTOS, J. R. MORALES, AND M. A. SANTOS (2019): "Impact of the 2017 Sanctions on Venezuela: Revisiting the Evidence," Tech. rep., Brookings Institution.

BELLORÍN, C. (2016): "El Furrial: The Spectacular Decline of a Giant Oil Field," Caracas Chronicles, 28 July 2016. Documents the 1998 El Furrial high-pressure gas-injection plant (IGF) operated by the Williams–Exterran consortium Wilpro, its 2009 expropriation, and the field's decline from 408,000 b/d in 2008 to 198,000 b/d in 2015.

BERG, R. C. (2021): "The Role of the Oil Sector in Venezuela's Environmental Degradation and Economic Rebuilding," Center for Strategic and International Studies (CSIS), 12 October 2021. Reports the volume of flared gas rising despite dramatic losses in oil production as the sector lost capacity to collect and reinject gas; deferred maintenance (a Punta Cardón facility uninspected since 2016) and the loss of technical staff; and an estimated $8 billion needed for pipeline infrastructure alone.

BLOOM, N., M. SCHANKERMAN, AND J. VAN REENEN (2013): "Identifying Technology Spillovers and Product Market Rivalry," *Econometrica*, 81, 1347–1393.

BLUNDELL, W. AND A. KOKOZA (2022): "Natural Gas Flaring, Respiratory Health, and Distributional Effects," *Journal of Public Economics*, 208, 104601.

CARACAS CHRONICLES (2024): "Dissecting the Muscar Explosion," Caracas Chronicles, 11 December 2024. Reports that light crude from northern Monagas is blended with Orinoco extra-heavy crude to produce the Merey 16 export grade, that PDVSA cut Orinoco output when light-crude diluent ran short, that the El Furrial-axis reinjection compressors (Pigap I and II) have been out of service for years, and that associated gas the compressors cannot reinject is flared or vented.

CHANG, T. (1998): "Upgrading And Refining Essential Parts Of Orinoco Development," Oil & Gas Journal, 19 October 1998.

CHÁVEZ ALAVA, A. AND R. VAZ (2021): "China's CNPC Set to Jumpstart Joint Oil Ventures in Venezuela," Venezuelanalysis, 4 September 2021 (updated 3 September 2023). Identifies the CNPC–PDVSA joint ventures (Sinovensa, Sinovenezolana I and II, Petrourica, Petrozumano) and reports that Sinovensa blends extra-heavy Orinoco crude into the Merey grade for export.

CONGRESSIONAL RESEARCH SERVICE (2024): "Venezuela: Overview of U.S. Sanctions," Tech. Rep. IF10715, CRS.

COULOMB, R., F. HENRIET, AND L. REITZMANN (2026): "'Bad' Oil, 'Worse' Oil and Carbon Misallocation," *Review of Economic Studies*, 93, 404–437.

COVERT, T. R. AND R. KELLOGG (2025): "Environmental Consequences of Hydrocarbon Infrastructure Policy," Working Paper 23855, National Bureau of Economic Research, conditionally accepted, *Journal of Political Economy*.

CROZET, M. AND J. HINZ (2020): "Friendly Fire: The Trade Impact of the Russia Sanctions and Counter-Sanctions," *Economic Policy*, 35, 97–146.

CUST, J., D. MANLEY, AND G. CECCHINATO (2017): "Unburnable Wealth of Nations," *Finance & Development*, 54.

DUFLO, E., M. GREENSTONE, R. PANDE, AND N. RYAN (2018): "The Value of Regulatory Discretion: Estimates from Environmental Inspections in India," *Econometrica*, 86, 2123–2160.

FERNÁNDEZ-VILLAVERDE, J., Y. LI, L. XU, AND F. ZANETTI (2025): "Charting the Uncharted: The (Un)Intended Consequences of Oil Sanctions and Dark Shipping," Working Paper 33486, National Bureau of Economic Research.

FIORETTI, M., J. HE, AND J. TAMAYO (2026a): "Capacity, Technology Portfolios, and the Paradox of Concentration," CEPR Discussion Paper 21607, CEPR Press.

FIORETTI, M., A. IARIA, A. JANSSEN, C. MAZET-SONILHAC, AND R. K. PERRONS (2026b): "Sovereign Hold-Up and Technology Adoption: Evidence from the North Sea," Working Paper.

FOWLIE, M., S. P. HOLLAND, AND E. T. MANSUR (2012): "What Do Emissions Markets Deliver and to Whom? Evidence from Southern California's NOx Trading Program," *American Economic Review*, 102, 965–993.

GILROY, T., L. S. TEST, AND A. TOVAR (2022): "OFAC Issues Venezuela General License Authorizing Chevron to Resume Limited Extraction Operations," Global Sanctions and Export Controls Blog, Baker McKenzie, 2 December 2022. General License 41 (26 November 2022) authorizes the production, lifting, and related maintenance, repair, and servicing of the Chevron joint ventures and the purchase of diluents and condensates, while prohibiting payments of taxes, royalties, or dividends to the Government of Venezuela or PDVSA and any expansion beyond fields operational as of 28 January 2019.

GRAFF, T. (2026): "Depreciation and Growth: Evidence from Machine Repair in Uganda," Job Market Paper, Harvard University.

GRÜNBERGER, F. (2025): "Venezuelan Supply and Export Scenarios Under a US Military Intervention," Kpler, 2 December 2025. Reports that Venezuela's diluent for blending Orinoco extra-heavy crude rotated from Iranian condensate (2020–2023) to US naphtha (January 2023–May 2025) to Russian naphtha (second half of 2025), that diluent access is the main supply bottleneck, and that upstream operations fall if diluent imports stop for more than six weeks.

GUGARATS, H. (2024): "US Extends Oil Service Firms' Venezuela Waiver," Argus Media, 7 November 2024. The four oilfield-service firms (Halliburton, SLB, Baker Hughes, Weatherford) are allowed to pay staff and maintain limited operations but barred from drilling new wells or otherwise contributing to PDVSA production and exports.

GUTMANN, J., M. NEUENKIRCH, AND F. NEUMEIER (2023): "The Economic Effects of International Sanctions: An Event Study," *Journal of Comparative Economics*, 51, 1214–1231.

HAJDARI, U. (2025): "Explainer: Why Chevron Still Operates in Venezuela Despite US Sanctions," Euronews, 29 December 2025. Reports that Chevron's spending covers basic operating costs—staff, maintenance, and transport—for between a quarter and a third of Venezuela's oil production, with the licence structured so cash does not reach the state.

HERNÁNDEZ, I. AND F. MONALDI (2016): "Weathering Collapse: An Assessment of the Financial and Operational Situation of the Venezuelan Oil Industry," CID Working Paper 327, Center for International Development at Harvard University, Cambridge, MA.

HSIEH, C.-T. AND P. J. KLENOW (2009): "Misallocation and Manufacturing TFP in China and India," *Quarterly Journal of Economics*, 124, 1403–1448.

HUFBAUER, G. C., J. J. SCHOTT, K. A. ELLIOTT, AND B. OEGG (2007): *Economic Sanctions Reconsidered*, Peterson Institute for International Economics, 3rd ed.

IMBENS, G. W. AND M. KOLESÁR (2016): "Robust Standard Errors in Small Samples: Some Practical Advice," *Review of Economics and Statistics*, 98, 701–712.

INCORRYS (2026): "The Bottleneck for Venezuelan Oil Industry," Incorrys Inc., 12 January 2026. Notes that Orinoco extra-heavy crude must be blended with a lighter hydrocarbon (naphtha, condensate, or light crude); that associated gas from light and medium oil fields is mostly flared for lack of infrastructure for capture and processing; and that scaling production would require significant investment in gas production, gas transportation, and steam-generation infrastructure (boilers, gas pipelines to heavy-oil fields, and gas-handling facilities).

INTERNATIONAL ENERGY AGENCY (2025): "Global Methane Tracker 2025," Tech. rep., IEA.

KENNEDY, S. (2026): "Venezuela's Gas: The World's Most Expensive Bonfire," Energy Flux, 15 January 2026. Documents large-scale flaring and methane venting across the Maracaibo basin and the Orinoco Belt, deteriorating gas-transmission pipelines, and Monagas flares visible from space.

LADE, G. E. AND I. RUDIK (2020): "Costs of Inefficient Regulation: Evidence from the Bakken," *Journal of Environmental Economics and Management*, 102, 102336.

LAUVAUX, T., C. GIRON, M. MAZZOLINI, A. D'ASPREMONT, R. DUREN, D. CUS-

WORTH, D. SHINDELL, AND P. CIAIS (2022): "Global Assessment of Oil and Gas Methane Ultra-Emitters," *Science*, 375, 557–561.

LORENTE, A., T. BORSDORFF, A. BUTZ, O. HASEKAMP, J. DE BRUGH, A. SCHNEIDER, L. WU, F. HASE, R. KIVI, D. WUNCH, D. F. POLLARD, K. SHIOMI, N. M. DEUTSCHER, V. A. VELAZCO, C. M. ROEHL, P. O. WENNBERG, T. WARNEKE, AND J. LANDGRAF (2021): "Methane Retrieved from TROPOMI: Improvement of the Data Product and Validation of the First 2 Years of Measurements," *Atmospheric Measurement Techniques*, 14, 665–684.

LORENTE, A., T. BORSDORFF, M. C. MARTINEZ-VELARTE, A. BUTZ, O. P. HASEKAMP, L. WU, AND J. LANDGRAF (2022): "Evaluation of the Methane Full-Physics Retrieval Applied to TROPOMI Ocean Sun Glint Measurements," *Atmospheric Measurement Techniques*, 15, 6585–6603.

LYON, D. R., B. HMIEL, R. GAUTAM, M. OMARA, K. A. ROBERTS, Z. R. BARKLEY, K. J. DAVIS, N. L. MILES, V. C. MONTEIRO, S. J. RICHARDSON, S. CONLEY, M. L. SMITH, D. J. JACOB, L. SHEN, D. J. VARON, A. DENG, X. RUDELIS, N. SHARMA, K. T. STORY, A. R. BRANDT, M. KANG, E. A. KORT, A. J. MARCHESE, AND S. P. HAMBURG (2021): "Concurrent variation in oil and gas methane emissions and oil price during the COVID-19 pandemic," *Atmospheric Chemistry and Physics*, 21, 6605–6626.

MACKINNON, J. G. AND M. D. WEBB (2018): "The Wild Bootstrap for Few (Treated) Clusters," *The Econometrics Journal*, 21, 114–135.

MARKS, L. (2022): "The Abatement Cost of Methane Emissions from Natural Gas Production," *Journal of the Association of Environmental and Resource Economists*, 9, 165–198.

MASNADI, M. S., H. M. EL-HOUJEIRI, D. SCHUNACK, Y. LI, J. G. ENGLANDER, A. BADAHDAH, J.-C. MONFORT, J. E. ANDERSON, T. J. WALLINGTON, J. A. BERGERSON, ET AL. (2018): "Global Carbon Intensity of Crude Oil Production," *Science*, 361, 851–853.

MOGOLLON, M. (2021): "Commodities 2021: Venezuela's Oil Industry Expected to Deteriorate Further," S&P Global Platts, 4 January 2021, Caracas. Reports active drill rigs at zero in Oct–Nov 2020; El Furrial among eastern fields with declining activity; the Paraguaná Refining Center at 13.2% of its 955,000 b/d capacity; "growing operating expenses and the deepening deterioration of energy assets.".

MONALDI, F., I. HERNÁNDEZ, AND J. LA ROSA REYES (2021): "The Collapse of the Venezuelan Oil Industry: The Role of Above-Ground Risks Limiting Foreign Investment," *Resources Policy*, 72, 102116.

NATHAN, B., J. D. MAASAKKERS, S. NAUS, R. GAUTAM, M. OMARA, D. J. VARON, M. P. SULPRIZIO, L. A. ESTRADA, A. LORENTE, T. BORSDORFF, R. J. PARKER, AND I. ABEN (2024): "Assessing Methane Emissions from Collapsing Venezuelan

Oil Production Using TROPOMI," *Atmospheric Chemistry and Physics*, 24, 6845–6863.

NEUENKIRCH, M. AND F. NEUMEIER (2015): "The Impact of UN and US Economic Sanctions on GDP Growth," *European Journal of Political Economy*, 40, 110–125.

ONSAT, J. (2024): "PDVSA–Chevron JV Launches Venezuela 2024 Drilling Campaign," Rigzone, 5 April 2024. Chevron's Petroindependencia joint venture resumed operations under General License 41, beginning a drilling campaign in the Carabobo block at fields operational before the sanctions.

PLANT, G., E. A. KORT, L. T. MURRAY, J. D. MAASAKKERS, AND I. ABEN (2022): "Evaluating urban methane emissions from space-based observations," *Remote Sensing of Environment*, 268, 112756.

PUSTEJOVSKY, J. E. AND E. TIPTON (2018): "Small-Sample Methods for Cluster-Robust Variance Estimation and Hypothesis Testing in Fixed Effects Models," *Journal of Business & Economic Statistics*, 36, 672–683.

RESTUCCIA, D. AND R. ROGERSON (2008): "Policy Distortions and Aggregate Productivity with Heterogeneous Establishments," *Review of Economic Dynamics*, 11, 707–720.

RODRÍGUEZ, F. R. (2022): "Sanctions, Economic Statecraft, and Venezuela's Crisis," Tech. rep., Sanctions & Security Research Project / Fourth Freedom Forum.

SHAPIRO, J. S. AND R. WALKER (2018): "Why Is Pollution from US Manufacturing Declining? The Roles of Environmental Regulation, Productivity, and Trade," *American Economic Review*, 108, 3814–3854.

TOMBE, T. AND J. WINTER (2015): "Environmental Policy and Misallocation: The Productivity Effect of Intensity Standards," *Journal of Environmental Economics and Management*, 72, 137–163.

TRUE, W. R. (1998): "Orinoco Projects Choose Dilution To Move Production," Oil & Gas Journal, 19 October 1998.

U.S. DEPARTMENT OF THE TREASURY, OFFICE OF FOREIGN ASSETS CONTROL (2025): "Venezuela General License No. 41B: Authorizing the Wind Down of Certain Transactions Related to Chevron Corporation's Joint Ventures," Issued 24 March 2025; wound Chevron's Venezuela joint-venture operations down through 27 May 2025.

U.S. ENERGY INFORMATION ADMINISTRATION (2024): "Country Analysis Executive Summary: Venezuela," Tech. rep., EIA.

U.S. ENVIRONMENTAL PROTECTION AGENCY (2023): "Report on the Social Cost of Greenhouse Gases: Estimates Incorporating Recent Scientific Advances," Tech. rep., U.S. Environmental Protection Agency.

WEISBROT, M. AND J. D. SACHS (2019): "Punishing Civilians: U.S. Sanctions on Venezuela," *Challenge*, 62, 299–321.

WORLD BANK (2024): "Global Gas Flaring Tracker Report," Tech. rep., World Bank Group, Global Gas Flaring Reduction Partnership.

——— (2025): "Global Gas Flaring Tracker Report," Tech. rep., World Bank Group, Global Gas Flaring Reduction Partnership.

——— (2026): "Global Gas Flaring Tracker Report," Tech. rep., World Bank Group, Global Flaring and Methane Reduction Partnership, june 2026 release; enhanced methodology using three NOAA satellites and a recalibrated flare-location catalog (with the Payne Institute, Colorado School of Mines).

Online Appendix

The two-field model (Appendix A) and the record-linkage procedure (Appendix B) come first, followed by supplementary and robustness exhibits for the composition (Appendix C) and strain (Appendix D) channels.

A A Two-Field Model of Reallocation Under Sanctions

This appendix formalizes the three channels of Section 2 in the simplest two-field economy in which a sanctions-induced rise in per-field fixed costs endogenously concentrates surviving production on one field. On that composition margin we layer the maintenance and strain margins, recovering the damage function of Equation (1). The model defines what each channel is and shows how one fixed-cost shock activates all three; it is not estimated.

Setup. A producer operates two fields $i \in \{S, L\}$ with capacities $Q_S < Q_L$, constant marginal costs $c_S < c_L$, and per-barrel damage intensities α_S, α_L; which of the two is dirtier is left open. Field i's environmental damage is

$$D_i \;=\; \alpha_i(m_i)\, q_i \;+\; \tfrac{\beta_i}{2}\, q_i^2,$$

its per-barrel intensity $\alpha_i(m_i) = \alpha_i^0\, g(m_i)$, falling in the maintenance budget m_i (with $g(0) = 1$, $g' < 0$, $g'' > 0$), times output q_i, plus a convex term ($\beta_i \geq 0$) that grows as output presses against the field's fixed gas-handling capacity. Operating a field costs a per-period fixed cost F. The producer takes the world price p as given and must raise revenue G, so it must produce $q^* \equiv G/p$, which it does at least cost. We assume $Q_S < q^* < Q_L$: the small field alone cannot meet the target; the large field alone can.

Composition: the reallocation threshold. Two production plans meet the target. Running both fields ($q_S = Q_S$, $q_L = q^* - Q_S$) costs $c_S Q_S + c_L(q^* - Q_S) + 2F$; running only the large field ($q_S = 0$, $q_L = q^*$) costs $c_L q^* + F$. Running both is cheaper if and only if

$$F \;<\; (c_L - c_S)\, Q_S,$$

that is, when the fixed cost of a second field falls short of the variable-cost penalty of routing its Q_S barrels through the dearer field instead. Sanctions scale the fixed cost, $F \mapsto \lambda F$ with $\lambda > 1$ (evasion overhead, parts substitution, foreign-expertise sourcing). The small field is retired once $\lambda F > (c_L - c_S)Q_S$, i.e. once

$$\lambda \;>\; \lambda^* \;\equiv\; \frac{(c_L - c_S)\, Q_S}{F}.$$

The threshold λ^* is lower, so a field is retired more readily, the larger its fixed cost relative to the marginal-cost gap it saves; mature, high-overhead fields cross first. This is the *composition* margin: the operating set shrinks from $\{S, L\}$ to $\{L\}$ and Q_S barrels move to the survivor. Whether that raises or lowers aggregate intensity depends on the sign of $\alpha_L - \alpha_S$, which the threshold does not pin down; Section 5 finds the retired fields to be the dirtier ones, so composition *lowers* average intensity, an offset.

Maintenance and strain: the within-field margins. The same shock moves two margins at the survivor L. Sanctions raise the cost of imported parts and contractors and so lower the chosen m_L; since $g' < 0$, the smaller budget raises the per-barrel intensity $\alpha_L(m_L)$, the *maintenance* margin. And the Q_S barrels that the survivor absorbs push q_L up the convex term, so damage per barrel rises faster than output, the *strain* margin, by more the closer q_L runs to capacity. The survivor's per-barrel intensity changes by

$$\Delta\iota_L \;=\; \underbrace{\alpha_L^0\, g'(m_L)\, \Delta m_L}_{\text{maintenance} > 0} \;+\; \underbrace{\tfrac{\beta_L}{2}\, \Delta q_L}_{\text{strain} > 0},$$

both terms positive when sanctions cut upkeep ($\Delta m_L < 0$) and concentrate output ($\Delta q_L > 0$).

Decomposition. Aggregate per-barrel intensity is the production-weighted average $I = \sum_i s_i\, \iota_i$, with production shares s_i and field intensities $\iota_i = \alpha_i(m_i) + \frac{\beta_i}{2} q_i$. A change in I splits into a between-field term, the shift in the operating set and shares (composition), and a within-field term $\Delta\iota_L$ (maintenance plus strain). That split is the shift-share that Section 5 estimates. The model's lesson is that one fixed-cost shock activates all three margins at once, so no single pollution series identifies them; recovering each requires a design that holds two fixed while moving the third, the strategy of Sections 5 to 7.

B Linking Flaring, Production, and Methane Records

The three spatial records are joined by location, and how they are joined determines what each regression can identify. This appendix sets out the procedure summarized in Section 4.

Flaring to fields. We link World Bank VIIRS flare-site-years to Rystad fields in two steps. Accepted flare-site name matches are assigned directly to their field in years when that field is producing; remaining site-years are allocated across producing fields inside a geographic buffer using production-weighted inverse-squared-distance weights with a 100-meter floor, falling back to pure inverse-squared-distance weights when production is missing, and the allocated flare volume divided by Rystad production gives flaring per barrel. The buffer radius trades one error against another: too tight, and a field's flares fall outside it and are lost; too loose, and they are shared with neighbors that did not produce them. Because oil-field infrastructure extends several kilometers from the reported centroid, and a satellite flare need not sit at that centroid, too tight a radius systematically drops valid matches. Appendix Figure B.1 is a representative case: Acema A, whose name-confirmed flare site lies 14.6 km from its Rystad centroid, outside a 7.5 km buffer but inside the 15 km default.

Methane to activity. We tag each TROPOMI cell by what sits near it. A cell is a wellhead cell if a field of a given type lies within 20 km, and a corridor cell if a pipeline passes near it but no wellhead does, the pipeline network being the union of the OpenStreetMap and Global Energy Monitor layers; cells far from any field or pipe are the background. Corridor cells are split between the two systems by comparing distance to the Faja extra-heavy family and the conventional-eastern family, with a 150 km cap: the heavy-crude corridor is closer to the Faja family, and the conventional-crude corridor to the conventional-eastern family. Cells near the Maracaibo fields that fall over the open lake are excluded from that class, because the TROPOMI methane column is retrieved reliably only over land and over the ocean in sun-glint geometry, so open-water retrievals are unreliable (Lorente et al., 2022). The naphtha price enters as a single national series, the northwest-European spot benchmark, common to every Venezuelan cell in a given month.

These links let a field's production, the flares above it, the methane column over its corridors, and the world price of its diluent enter one regression together. The distinct geography of flares (point sources at the wellhead) and methane (diffuse, along the corridor) is why the flaring and venting channels are estimated on different cuts of the data.

Figure B.1: Flare allocation and the buffer radius: a field missed at 7.5 km, captured at 15 km

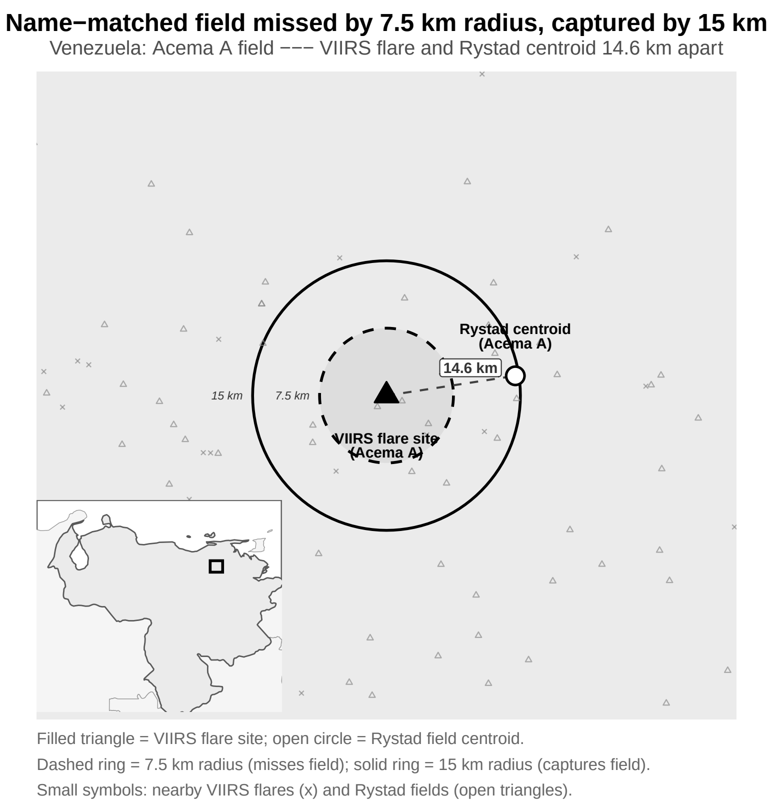

Notes. Acema A, Venezuela. The filled triangle is the World Bank VIIRS flare-site location and the open circle the Rystad field centroid; fuzzy name matching confirms both refer to the same field, yet their coordinates are 14.6 km apart. The dashed allocation ring is the 7.5 km buffer and the solid ring the 15 km buffer: at 7.5 km the centroid falls outside the buffer and the field would be dropped from the distance-based allocation. Small grey symbols mark other nearby VIIRS flare sites (×) and Rystad centroids (open triangle, △); the inset locates the area within Venezuela. Flare-site locations are from World Bank VIIRS and field centroids from Rystad UCube. Basemap from Natural Earth.

Table B.1: The sanctions difference-in-differences on production, spending, and flaring

Outcome	Venezuela $\times$ Post	Observations
Flaring volume, log (10 km)	-0.135^{***}	19,360
	(0.050)	
Flaring volume, log (15 km)	-0.121^{**}	19,360
	(0.049)	
Flaring intensity (10 km)	$+45.128^{***}$	19,360
	(13.657)	
Flaring intensity (15 km)	$+53.477^{***}$	19,360
	(14.627)	
Production, log	-0.604^{***}	19,360
	(0.111)	
OPEX, log	-0.514^{***}	19,360
	(0.116)	
CAPEX, log	-0.344	19,360
	(0.244)	
Field, year FE	Yes	

Notes. The difference-in-differences behind Figure 2: all Venezuelan fields against the five comparison countries, on the six-country field-year panel, 2012–2024, with Post $= \mathbb{1}\{\text{year} \geq 2017\}$. Standard errors, clustered by field, are in parentheses. Columns 1–4 report flared volume and flaring intensity under the 10 and 15 km allocation rules; intensity is winsorized at the 99.5th percentile. Volume, production, and spending enter in logs. $^{***}p < 0.01$, $^{**}p < 0.05$, $^{*}p < 0.10$.

C The Composition Channel

This appendix documents the composition-channel exhibits in full, giving for each regression its specification, fixed effects, and standard errors, and discussing its result. The composition channel is the between-field term of the decomposition in Equation (3): the change in aggregate flaring intensity that follows from the shift in which fields produce, holding each field's own per-barrel intensity at its pre-sanctions level. The exhibits establish two facts. First, that term is negative, so the reallocation of output across fields lowered aggregate intensity and offset part of the within-field rise rather than causing it. Second, the fields that kept producing were the resource-rich, foreign-operated ones, selected on their resource base and their operator rather than on their past output.

Figure C.1: Size-gradient event study for the composition difference-in-differences

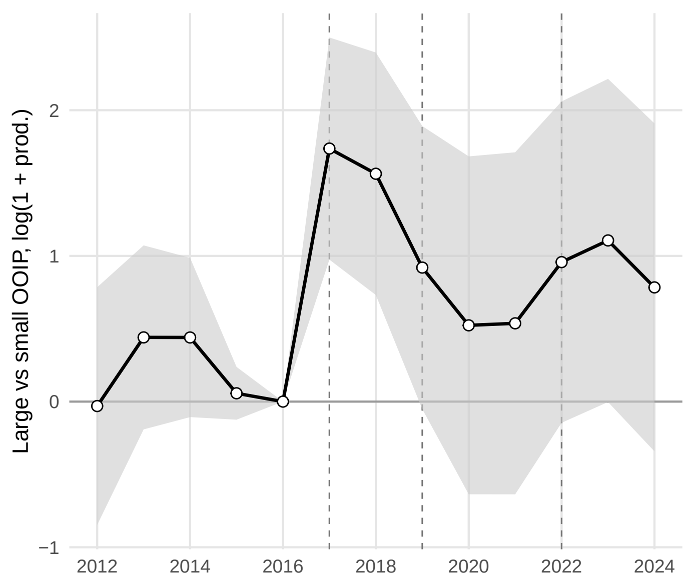

Notes. Year coefficients, with 2016 as the omitted reference year, from a regression of $\log(1 + \text{field-level production})$ on year indicators interacted with an above-median oil-in-place indicator, within Venezuela, with field and year fixed effects and 95% confidence bands from standard errors clustered by field. This is the size gradient of columns 2 and 4 of Table 2. Vertical dashed lines mark the 2017, 2019, and 2022 sanctions tightenings. Production and oil-in-place are from Rystad UCube.

Which fields kept producing. Appendix Figure C.1 traces the production gap between large- and small-resource Venezuelan fields over time. It plots the coefficients from a regression of $\log(1 + \text{production}_{it})$ on year indicators interacted with an indicator for above-median oil-in-place, estimated on Venezuelan fields with field and year fixed effects and 2016 as the omitted reference year; the bands are 95 percent confidence intervals with standard errors clustered by field. The field effects absorb every time-invariant difference between fields and the year effects every shock common to a year, so the coefficients isolate how the large-minus-small production gap moves relative to 2016. The pre-sanctions coefficients are flat and insignificant, and the gap opens only after 2017, so the resource-size gradient in columns 2 and 4 of Table 2 is a break at the sanctions rather than the continuation of a prior trend.

Appendix Table C.1 runs the candidate margins against one another on a Venezuela-only cross-section of the 227 fields active before 2017. The outcome is the single long change in $\log(1 + \text{production})$ between the 2012–2016 and 2022–2024 means, so there is one observation per field, the regression carries no fixed effects, and the standard errors are heteroskedasticity-robust. The regressors are the field's log oil-in-place, log pre-period production, age, pre-period flaring intensity, and an indicator that its foreign operator kept operating through the sanctions (Chevron, CNPC, Rosneft, or ONGC). Entered together, the resource base and the operator predict retention, at $+0.25$ to $+0.29$ for log oil-in-place and $+1.04$ for operator-stayed, each significant at five percent, while past production, field age, and prior flaring intensity do not. The two surviving margins are related in the data, the nine operator-stayed fields holding a median 7,414 mn barrels of oil in place against 125 mn for the rest, which is why Appendix Table C.5 separates them.

Appendix Table C.2 examines the same selection from the closure side. It is a logit, with one observation per field and therefore no fixed effects, of an indicator that the field is inactive or nearly inactive by the post-period on log pre-period production and log oil-in-place, with heteroskedasticity-robust standard errors, estimated first across Latin America (1,689 fields) and then on Venezuela alone (229). Across Latin America both margins predict survival (-0.26 and -0.29, each $p < 0.01$). Within Venezuela only the resource base does: log oil-in-place enters at -0.19 ($p < 0.10$) and past production is essentially zero (-0.01), so closure in Venezuela sorted on resources rather than on incumbency.

Appendix Table C.3 checks that the cross-country size gradient is not an artifact of comparing Venezuela to dissimilar controls. Columns 1 and 3 reproduce the Latin-

Table C.1: Which Venezuelan fields held their output: resources, operator, and past production

	Outcome: change in log(1 + production): between 2012–16 and 2022–24		
	(1)	(2)	(3)
Log pre-period production (production size)	$+0.05$	-0.13	-0.12
	(0.04)	(0.09)	(0.09)
Log oil in place (resource size)		$+0.29^{**}$	$+0.25^{**}$
		(0.12)	(0.12)
Field age (years since start-up)		-0.00	-0.00
		(0.01)	(0.01)
Pre-period flaring intensity (log)			$+0.01$
			(0.02)
Foreign operator stayed			$+1.04^{**}$
			(0.49)
Venezuelan fields	227	227	227

Notes. Cross-section of the 227 Venezuelan fields active before 2017. The outcome is the change in $\log(1 + \text{annual production})$ between the 2012–2016 and 2022–2024 means, so there is one observation per field and the regression carries no fixed effects. Heteroskedasticity-robust standard errors are in parentheses. "Foreign operator stayed" marks the fields whose partner kept operating through the sanctions (Chevron, CNPC, Rosneft, ONGC). $^{***}p < 0.01$, $^{**}p < 0.05$, $^{*}p < 0.10$.

Table C.2: Which fields shut down: closure on size and resources

	(1) All Latin America	(2) Venezuela only
Outcome: field is inactive or nearly inactive by the post-period		
Log pre-period production	-0.26^{***}	-0.01
	(0.04)	(0.09)
Log oil in place	-0.29^{***}	-0.19^{*}
	(0.05)	(0.12)
Fields	1689	229

Notes. Logit of an indicator that the field is inactive by the post-period on log pre-period (2012–2016) production and log oil in place. Heteroskedasticity-robust standard errors are in parentheses. $^{***}p < 0.01$, $^{**}p < 0.05$, $^{*}p < 0.10$.

American columns of Table 2, regressing $\log(1 + \text{production}_{it})$ on Post $\times$ Large, Post $\times$ PDVSA, and their triple with field and year fixed effects and field-clustered standard errors; columns 2 and 4 reweight the five comparison countries' fields toward Venezuela's covariate profile by stabilized inverse-probability weights, built from a propensity score in log pre-period production, log oil-in-place, and a heavy-crude indicator, trimmed to $[0.02, 0.98]$ with weights capped at the 99th percentile.

The two main effects survive the reweighting: the size gradient (Post $\times$ Large) runs from $+0.66$ to $+1.33$ and the PDVSA penalty (Post $\times$ PDVSA) from -1.21 to -2.21, each significant in all four columns. The triple does not. It is -1.03 ($p < 0.05$) in column 1, which measures size by pre-period production, and -0.53, -0.60, and -0.39, none significant, in the other three, including both columns that measure size by oil-in-place. The data therefore identify the two margins separately—resources and a foreign operator each predicted retention—more sharply than they identify the interaction between them. Two caveats apply. The effective control sample is thin, because few comparison fields resemble Venezuela's, and which partners stayed was not random.

Table C.3: Composition LATAM columns under inverse-probability weighting

	Dependent variable: log(1 + annual production)			
	(1)	(2)	(3)	(4)
Post $\times$ Large	$+1.12^{***}$	$+0.66^{*}$	$+1.33^{***}$	$+1.12^{***}$
	(0.16)	(0.39)	(0.16)	(0.31)
Post $\times$ PDVSA-owned	-1.21^{***}	-2.21^{***}	-1.41^{***}	-2.05^{***}
	(0.30)	(0.43)	(0.33)	(0.35)
$\times$ Large (triple)	-1.03^{**}	-0.53	-0.60	-0.39
	(0.47)	(0.60)	(0.47)	(0.54)
Large	pre-prod.	pre-prod.	OOIP	OOIP
IPW (Venezuela profile)	No	Yes	No	Yes
Field, year FE	Yes	Yes	Yes	Yes
Observations	21,970	21,554	21,957	21,554

Notes. Columns 1 and 3 reproduce the Latin-American columns of Table 2; columns 2 and 4 reweight the five comparison countries' fields toward Venezuela's covariate profile by stabilized inverse-probability weights. The production outcome is $\log(1 + \text{annual production})$. The propensity score is $\Pr(\text{Venezuela} \mid$ log pre-period production, log oil-in-place, and a heavy-crude indicator); scores are trimmed to $[0.02, 0.98]$ (2% of fields dropped) and weights capped at the 99th percentile (9.63). Standard errors, clustered by field, are in parentheses. $^{***}p < 0.01$, $^{**}p < 0.05$, $^{*}p < 0.10$.

The size of the offset. Appendix Table C.4 reports the shift-share decomposition of the per-barrel intensity rise across specifications. The between-field (composition) and within-field terms are an accounting split of the change in production-weighted aggregate intensity defined in Equation (3), so they carry no standard errors. Across the three pre/post windows and both VIIRS flaring-allocation buffers (10 and 15 km), the composition term stays between −5.25 and −7.17 m^3/bbl and the within-field term between +29.6 and +37.8, so the offset never changes sign, and the within-field rise is four to seven times its size in every cell. Appendix Table C.5 re-aggregates the same composition term by two overlapping groupings, ownership (foreign joint venture versus PDVSA-sole) and crude type (the extra-heavy Faja versus the rest), giving −3.57 and −4.03 against a total of −6.12. Both margins push in the same direction, so the offset runs through ownership and geology together, the surviving core being at once foreign-operated and gas-poor.

Table C.4: Composition decomposition under alternative windows and flaring buffers

	10 km buffer		15 km buffer	
Pre / post window	Composition	Within-field	Composition	Within-field
2012–16 / 2022–24 (baseline)	−7.17	+32.53	−6.89	+34.64
2012–14 / 2023–24 (wide)	−5.56	+29.64	−5.25	+31.55
2015–16 / 2022–23 (narrow)	−6.96	+35.26	−6.71	+37.77

Notes. Production-weighted shift-share of the per-barrel flaring-equivalent intensity rise (m^3/bbl). "Composition" is the between-field term $\sum_i \Delta s_i \, \iota_{i,\text{pre}}$; "Within-field" is $\sum_i s_{i,\text{post}} \Delta \iota_i$, with the interaction included. Columns vary the VIIRS flaring-allocation buffer (10 vs 15 km); rows vary the pre- and post-period windows.

Table C.5: The composition offset by margin: ownership and crude type

Decomposition margin	Contribution (m^3/bbl)
Total composition term	−6.12
attributable to the ownership margin (Foreign JV vs. PDVSA-sole)	−3.57
attributable to the crude-type margin (Heavy Faja vs. other)	−4.03

Notes. The composition shift-share term of Table C.4, re-aggregated to two grouping margins: by ownership (foreign joint ventures vs. PDVSA-sole) and by crude type (the extra-heavy Faja core vs. the rest). Each row is $\sum_g \Delta S_g \, \bar{\iota}_{g,\text{pre}}$ over the stated groups. The two margins do not sum to the total because the groupings overlap.

D The Strain Channel

This appendix reports the strain-channel exhibits in full, giving for each regression its specification, fixed effects, and standard errors. The strain channel is the convex term of the damage function in Equation (1): the gas that an underfunded diluent and gas-handling chain, run past the capacity it was built for, can no longer move, and that escapes uncombusted rather than being captured. Uncombusted gas is not detected by the flaring satellite, so the exhibits draw on two records: the VIIRS flaring series for the descriptive setting, and the TROPOMI methane column for the identification.

The turnover and the denominator. Appendix Figures D.1 and D.2 are descriptive group sums rather than regressions, and carry no standard errors. Each allocates a field's oil-in-place, or its allocated flared volume, to its operators in proportion to their equity shares, sums within international-partner group, and compares Venezuela with the average of Argentina, Colombia, and Ecuador. The Western majors' Venezuelan resource base contracts after 2017 as they exit, the Russian partners that stayed expand, and the Chinese hold flat; flaring falls at the departing majors and rises at the fields that absorbed their output, while the neighbor benchmark moves in neither direction. Appendix Figure D.3 indexes Venezuelan totals to 2012: production falls by about two-thirds while flared volume ends the period near its 2012 level.

The timing of the price response. Appendix Table D.1 estimates when the methane column responds to the naphtha price. Each column is a separate regression of Equation (4) that enters a single lag of the log price interacted with the six cell classes, with cell and year-month fixed effects and standard errors clustered by cell, on a common sample of 25,520 cell-months. Single lags are entered rather than a joint distributed lag because the price has first-order autocorrelation of about 0.9, which makes joint lag terms collinear and individually uninterpretable. The heavy-corridor loading is $+10.09$ contemporaneously and $+5.61$ at one month, then -1.78 at two and -4.09 at three, the reversal that Section 6.2 reads as deferred purchases followed by restocking. A future-price placebo, the $t+1$ lead conditional on the current and three lagged prices, enters at $+1.3$ ($p = 0.79$).

Figure D.1: Share-weighted oil-in-place by international-partner group, Venezuela versus the unsanctioned-neighbor average

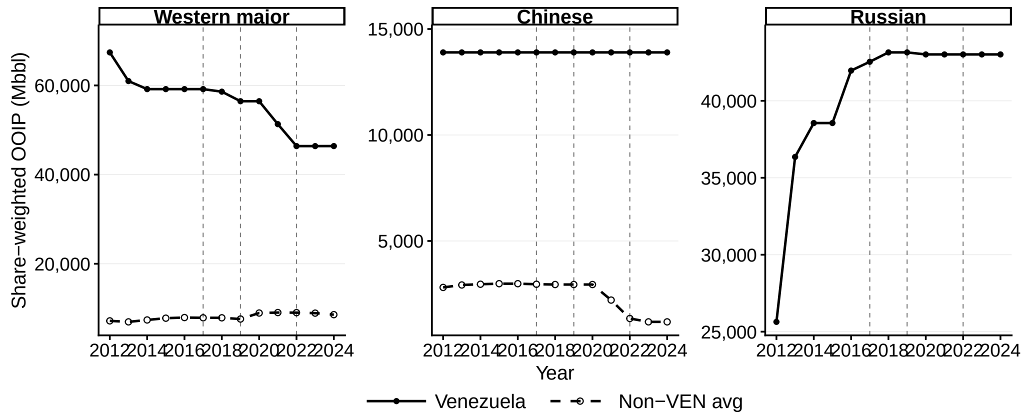

Notes. Each panel is one international-partner group: Western majors (including Chevron), Chinese, and Russian. Within a panel the solid line with filled markers is Venezuela and the dashed line with open markers is the average of Argentina, Colombia, and Ecuador. Each field's oil-in-place is allocated to its operators in proportion to their equity shares and summed within group, in million barrels; panels use a free vertical axis. Vertical dashed lines mark the 2017, 2019, and 2022 sanctions tightenings. Ownership shares and oil-in-place are from Rystad UCube.

Where the methane rose. Appendix Table D.2 regresses the log methane column on a per-year time trend interacted with a wellhead-area indicator—a cell within the stated radius of a pipeline and within 10 km of an oil or gas field—and further with a basin indicator, with standard errors clustered by cell; coefficients are the per-year change in the log column, multiplied by 10^3, against an omitted reference of wellhead-area cells in the five comparison countries lying in no heavy-oil basin. Venezuela's Orinoco Belt trends up at $+1.30$ a year ($p < 0.01$ at 20 km), Mexico's Maya down at -2.51, Colombia's Llanos at -0.81, and Ecuador's Oriente up at $+1.51$ on a profile of expansion rather than a sanctions shock.

Appendix Table D.3 localizes the rise within Venezuela. Panel B is a single pooled regression per column over 2,588,253 cell-months across the six countries, with cell and year-month fixed effects and standard errors clustered by cell, of the log column on a linear trend interacted with a Venezuela indicator, with a near-pipeline indicator, and with both. Venezuela's country-wide trend is -0.89 a year at 20 km and the near-pipeline trend in the comparison countries is -0.29, while the Venezuela-specific near-pipeline trend is $+0.88$ ($p < 0.01$) at every radius. Panel A estimates the near-pipeline trend within each group separately and obtains $+0.67$

Figure D.2: Allocated flaring volume by international-partner group, Venezuela versus the unsanctioned-neighbor average

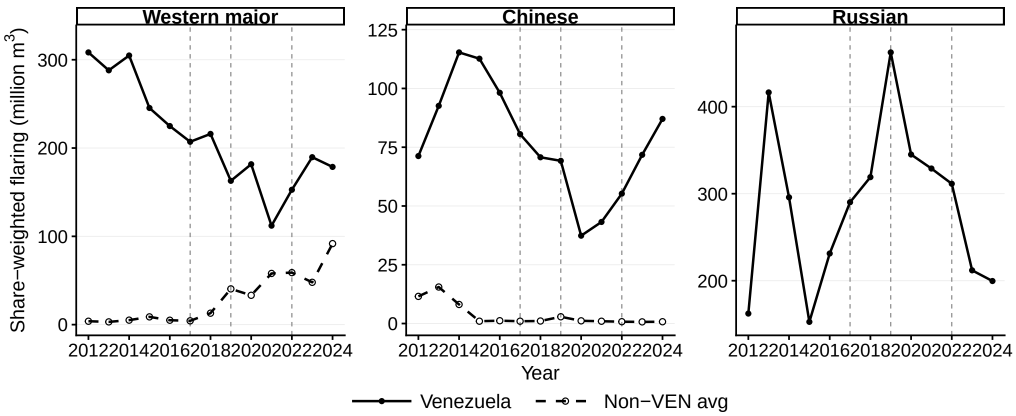

Notes. Each panel is one international-partner group: Western majors (including Chevron), Chinese, and Russian. Within a panel the solid line with filled markers is Venezuela and the dashed line with open markers is the average of Argentina, Colombia, and Ecuador. Each field-year's allocated flared volume is apportioned to its operators in proportion to their equity shares and summed within group, in million cubic meters; panels use a free vertical axis. Vertical dashed lines mark the 2017, 2019, and 2022 sanctions tightenings. Flaring is World Bank VIIRS volume allocated under the default 15 km field-allocation rule; ownership shares are from Rystad UCube.

Figure D.3: Flared volume changed far less than production: the per-barrel rise is the denominator

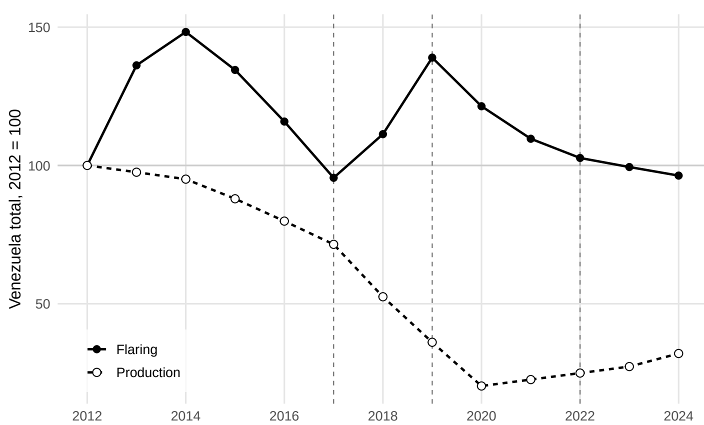

Notes. Venezuela totals indexed to 2012 $= 100$: satellite flared volume within the default 15 km field-allocation rule (solid line, filled markers) and oil production (dashed line, open markers). Vertical dashed lines mark the 2017, 2019, and 2022 sanctions tightenings. Flared volume is World Bank VIIRS; production is Rystad UCube.

inside Venezuela against -0.28 outside.

Corridor robustness. Appendix Table D.4 varies the fixed effects and the clustering at 20 km. The heavy-corridor loading is +10.09 in the baseline, +10.09 under two-way clustering by cell and month (standard error 4.48), +11.69 under a cell-specific calendar-month effect, +9.92 under a region-by-year-month effect, and +17.82 dropping the pandemic years. The conventional-corridor placebo is small and insignificant in every column but one: under the cell-seasonal effect it reaches +3.47 ($p < 0.01$), about a third of the heavy-corridor loading in that column. The gap between the two corridors, on which the design rests, is 8.8 in the baseline and 8.2 there.

Appendix Figure D.4 reassigns the corridor label to a random set of cells of the same size 999 times with the fixed effects held; the observed loading lies beyond every draw (permutation $p = 0.001$). Appendix Table D.5 varies the geography: widening the radius that defines a corridor cell raises the loading from +4.8 at 10 km to +10.2 at 20 and +13.4 at 50 (Panel A), and dropping corridor cells within 30, 40, and 50 km of any wellhead leaves it at +9.8, +9.9, and +11.1 (Panel B). Appendix Table D.6 drops the Maracaibo cells, whose negative loading Section 6.2 attributes to the lake complex: the heavy corridor is +9.78 at 20 km against +10.15, the Maturín wellheads +3.33 against +3.41, each retaining its significance, and the two predicted nulls remain null. Dropping the whole region, which also removes the open-lake cells that otherwise sit in the background reference, leaves the corridor at +9.58.

Table D.1: Naphtha-price lag structure for the heavy-crude corridor

	(1) Contemp.	(2) Lag-1	(3) Lag-2	(4) Lag-3
$\log(\text{Naphtha}_t) \times$ corridor	$+10.09^{***}$ (2.90)			
$\log(\text{Naphtha}_{t-1}) \times$ corridor		$+5.61^{*}$ (2.99)		
$\log(\text{Naphtha}_{t-2}) \times$ corridor			-1.78 (2.37)	
$\log(\text{Naphtha}_{t-3}) \times$ corridor				-4.09^{*} (2.31)
Cell fixed effects	Yes	Yes	Yes	Yes
Year-month fixed effects	Yes	Yes	Yes	Yes
Cell-months	25,520	25,520	25,520	25,520

Notes. Change in $\log(XCH_4)$, $\times 10^3$, per log point of the naphtha price, for cells in the 20 km heavy-crude pipeline corridor of Table 3. Each column is a separate regression that enters a single lag of the price interacted with the six cell classes of equation (4). Standard errors, clustered by cell, are in parentheses. $^{***}p < 0.01$, $^{**}p < 0.05$, $^{*}p < 0.10$.

Table D.2: Methane trend in wellhead-area cells, by heavy-oil basin

	Trend vs. the reference			Net basin trend		
Heavy-oil basin	10 km	20 km	50 km	10 km	20 km	50 km
Venezuela: the Orinoco Belt (extra-heavy)	$+1.57^{***}$	$+1.30^{***}$	$+1.15^{***}$	$+0.62$	$+0.39$	$+0.25$
Mexico: the Maya basin (heavy)	-2.34^{***}	-2.51^{***}	-2.65^{***}	-3.28	-3.43	-3.55
Colombia: the Llanos basin (heavy)	-0.73^{***}	-0.81^{***}	-0.82^{***}	-1.67	-1.73	-1.72
Ecuador: the Oriente basin (heavy)	$+1.38^{***}$	$+1.51^{***}$	$+1.68^{***}$	$+0.43$	$+0.60$	$+0.77$
Reference (LATAM, no heavy-oil basin)	-0.94^{***}	-0.92^{***}	-0.90^{***}			
Cell fixed effects	Yes					
Year-month fixed effects	Yes					
Wellhead-area cells (10 / 20 / 50 km)	2,090 / 3,141 / 4,276					

Notes. One regression per column-block of the log methane column on a per-year time trend interacted with a wellhead-area indicator (a cell within the stated radius of a pipeline and within 10 km of an oil or gas field), that interaction further interacted with a basin indicator. The estimate is the per-year change in the log column, multiplied by 10^3. Standard errors, clustered by cell, are in parentheses. The left block reports each basin's trend relative to the omitted reference, wellhead-area cells in the five comparison countries that lie in no heavy-oil basin; the right block adds the reference trend to give the net per-year trend in the basin. $^{***}p < 0.01$, $^{**}p < 0.05$, $^{*}p < 0.10$.

Figure D.4: Spatial placebo test for the heavy-crude corridor

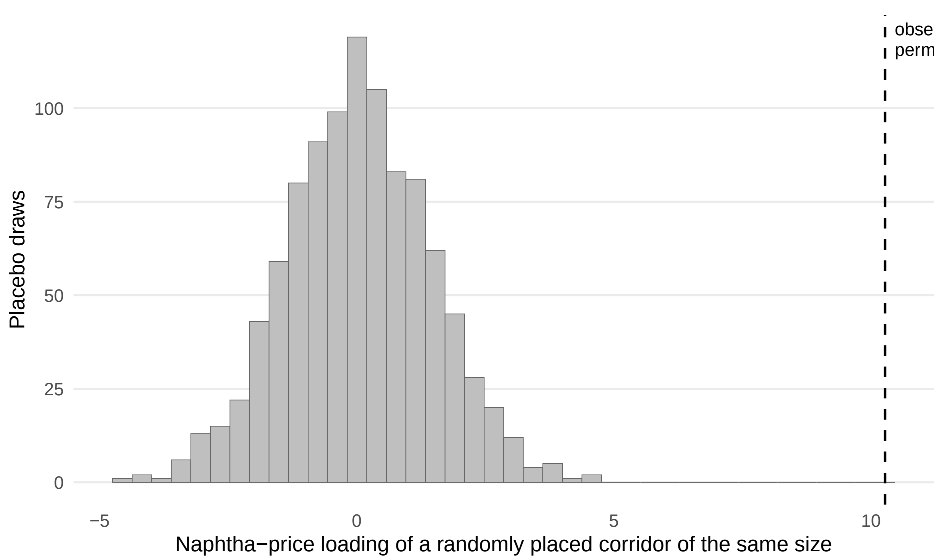

Notes. Distribution of the naphtha-price loading of the methane column when the corridor label is reassigned to a random set of cells of the same size (999 draws), holding cell and year-month fixed effects fixed. The dashed line marks the observed heavy-crude corridor loading; the permutation p-value is the share of placebo draws whose loading equals or exceeds it in absolute value. Methane is the Sentinel-5P TROPOMI column; the sample and specification are those of Table 3.

Table D.3: Is the methane rise country-wide in Venezuela, or only near pipelines?

	Near-pipe radius		
Per-year methane trend ($\times 10^3$)	10 km	20 km	50 km
A. Within-country near-pipe trend			
Venezuela, near a pipeline	$+0.78^{***}$	$+0.67^{***}$	$+0.47^{***}$
	(0.15)	(0.12)	(0.11)
Comparison countries, near a pipeline	-0.32^{***}	-0.28^{***}	-0.25^{***}
	(0.02)	(0.01)	(0.01)
B. Triple difference on the pooled panel			
Near a pipeline $\times$ Venezuela	$+1.03^{***}$	$+0.88^{***}$	$+0.72^{***}$
	(0.17)	(0.14)	(0.12)
Venezuela, country-wide	-0.81^{***}	-0.89^{***}	-1.06^{***}
	(0.07)	(0.07)	(0.09)
Near a pipeline, comparison baseline	-0.32^{***}	-0.29^{***}	-0.26^{***}
	(0.02)	(0.01)	(0.01)
Cell fixed effects	Yes	Yes	Yes
Year-month fixed effects	Yes	Yes	Yes
Venezuelan near-pipe cells	231	371	705
Cell-months (pooled)	2,588,253	2,588,253	2,588,253

Notes. The dependent variable is the log methane column. Panel A reports the per-year near-pipeline trend estimated separately within Venezuela and within the five comparison countries (Argentina, Brazil, Colombia, Ecuador, Mexico). Panel B is a single pooled regression per column: $\log \mathrm{XCH}_4 = \xi_i + \tau_t + \psi_0\,(t \cdot \text{Venezuela}) + \psi_2\,(t \cdot \text{NearPipe}) + \psi_1\,(t \cdot \text{NearPipe} \cdot \text{Venezuela})$, with ξ_i and τ_t the cell and year-month fixed effects. Coefficients are the per-year change in the log column multiplied by 10^3. Standard errors, clustered by cell, are in parentheses. $^{***}p < 0.01$, $^{**}p < 0.05$, $^{*}p < 0.10$.

Table D.4: Strain estimates under alternative fixed effects and clustering (20 km radius)

Cell type	(1) Baseline	(2) Two-way cluster	(3) Cell-seasonal FE	(4) Region × month FE	(5) Drop COVID 2020–21
Heavy-crude pipeline corridor	$+10.09^{***}$	$+10.09^{**}$	$+11.69^{***}$	$+9.92^{***}$	$+17.82^{***}$
	(2.90)	(4.48)	(2.46)	(2.86)	(5.12)
Conventional-crude corridor (placebo)	$+1.30$	$+1.30$	$+3.47^{***}$	$+1.91$	$+2.16$
	(1.05)	(1.40)	(1.06)	(1.18)	(2.52)
Cells near the conventional fields (Maturín)	$+3.37^{*}$	$+3.37$	$+3.28^{*}$	$+4.72^{***}$	$+2.39$
	(1.75)	(2.31)	(1.81)	(1.71)	(3.56)
Cells near the Faja extra-heavy fields	$+1.69$	$+1.69$	$+2.15$	$+1.78$	$+5.19$
	(1.68)	(1.84)	(3.01)	(1.92)	(4.46)
Cells near the Maracaibo fields	-5.91^{***}	-5.91^{*}	-4.90^{***}	-3.02^{**}	-12.54^{***}
	(1.94)	(3.36)	(1.58)	(1.31)	(2.33)
Other Venezuelan fields	-1.24	-1.24	-1.37	-2.29^{***}	$+0.15$
	(0.79)	(1.50)	(1.12)	(0.87)	(2.49)
Cell fixed effects	Yes	Yes	Yes	Yes	Yes
Year-month fixed effects	Yes	Yes	Yes	Yes	Yes
Cell × calendar-month FE	No	No	Yes	No	No
Region × month FE	No	No	No	Yes	No
Cell-months	25,520	25,520	21,861	25,520	19,866

Notes. Naphtha-price loading on the methane column ($\hat{\kappa}_k \times 10^3$) at the 20 km radius, the specification of the middle column of Table 3, varying the fixed effects and clustering one at a time as indicated in the column headers and panel rows. Standard errors, clustered by cell, are in parentheses; column (2) clusters two-way by cell and month. $^{***}p < 0.01$, $^{**}p < 0.05$, $^{*}p < 0.10$.

Table D.5: The heavy-corridor response across radii and wellhead-distance cuts

Panel A. Corridor radius	10 km	20 km	50 km
Heavy-crude corridor loading	$+4.8$	$+10.2^{***}$	$+13.4^{***}$
Panel B. Dropping corridor cells within X km of any wellhead (20 km radius)	> 30 km	> 40 km	> 50 km
Heavy-crude corridor loading	$+9.8^{***}$	$+9.9^{***}$	$+11.1^{***}$

Notes. Naphtha-price loading of the heavy-crude pipeline corridor ($\times 10^3$), from the six-class model of Table 3. Panel A varies the radius that defines a corridor cell. Panel B drops corridor cells that lie within 30, 40, or 50 km of any wellhead. All regressions control for cell and year-month fixed effects. Standard errors, clustered by cell, are in parentheses. $^{***}p < 0.01$, $^{**}p < 0.05$, $^{*}p < 0.10$.

Table D.6: Strain estimates excluding the Maracaibo cells (companion to Table 3)

	Coefficient on $\log(\mathrm{XCH_4})$ ($\times 10^3$)		
Cell type	10 km	20 km	50 km
Oil-field cells (within the radius of a wellhead)			
Cells near the Faja extra-heavy fields	$+0.30$	$+1.36$	$+0.42$
	(2.58) [14]	(1.68) [41]	(1.42) [93]
Cells near the conventional fields (Maturín)	$+2.99^{*}$	$+3.33^{*}$	$+3.31^{*}$
	(1.72) [20]	(1.78) [26]	(1.76) [29]
Other Venezuelan fields	$+0.88$	-1.19	$+0.62$
	(1.89) [13]	(0.78) [32]	(0.68) [116]
Pipeline-corridor cells (near a line, away from any wellhead)			
Heavy-crude pipeline corridor	$+4.73$	$+9.78^{***}$	$+12.59^{***}$
	(3.35) [29]	(2.89) [50]	(2.65) [66]
Conventional-crude corridor	$+1.78$	$+1.23$	$+1.04$
	(1.46) [77]	(1.05) [123]	(0.86) [190]
Cell fixed effects	Yes	Yes	Yes
Year-month fixed effects	Yes	Yes	Yes
Cell-months	25,149	24,148	22,440
Cells	1,265	1,229	1,157

Notes. The specification of Table 3 with the Maracaibo class dropped from the model; the five remaining classes and the background reference are otherwise unchanged, and each class holds the same cells as in Table 3. Standard errors, clustered by cell, are in parentheses. $^{***}p < 0.01$, $^{**}p < 0.05$, $^{*}p < 0.10$.